C.P. No. 1292

C.P. No. 1292

PROCUREMENT EXECUTIVE, MINISTRY OF DEFENCE

AERONAUTICAL RESEARCH COUNCIL

CURRENT PAPERS

Some Results of Wind-Tunnel Tests on an Aerofoil Section (NPL 9510) Combining a 'Peaky' Upper Surface-Pressure Distribution with Rear Loading

by

D. J. Hall, V. G. Quincey and R. C. Lock,

Aerodynamics Division, NPL

LONDON: HER MAJESTY'S STATIONERY OFFICE

1974

PRICE 60p NET

C.P. No.1292*
July 1969

SOME RESULTS OF WIND-TUNNEL TESTS ON AN AEROFOIL SECTION (NPL 9510) COMBINING A 'PEAKY' UPPER SURFACE-PRESSURE DISTRIBUTION WITH REAR LOADING

- by -
D.J. Hall, V.G. Quincey and R.C. Lock,
Aerodynamics Division, NPL

SUMMARY

Some experimental results are presented for an 11% thick aerofoil, NPL 9510, designed to combine a region of shock-free supersonic flow over most of the upper surface with a substantial amount of rear loading; to alleviate adverse pressure gradients on the upper surface just ahead of the trailing edge a 0.5% thick blunt-base was used. The design aims were to a large extent achieved at $M = 0.79$, $C_L = 0.6$, representing at least a 10% increase in drag rise Mach number over a conventional section of the same thickness and lift coefficient; but separation margins at the design condition are very small and an undesirable 'drag creep' appears at lower Mach numbers.

---

*Replaces A.R.C.31 312

1. Introduction

In recent years considerable progress has been made in the design of aerofoils incorporating regions of effectively shock-free supersonic flow over part of the upper surface, with isentropic compression from a high velocity peak close behind the leading edge (local Mach number M up to 1.4) to a rear sonic point typically at about 40% of the chord; a successful early example of this type (NPL 9283) is quoted in Ref. 1, a figure from which is reproduced below (Sketch (a))

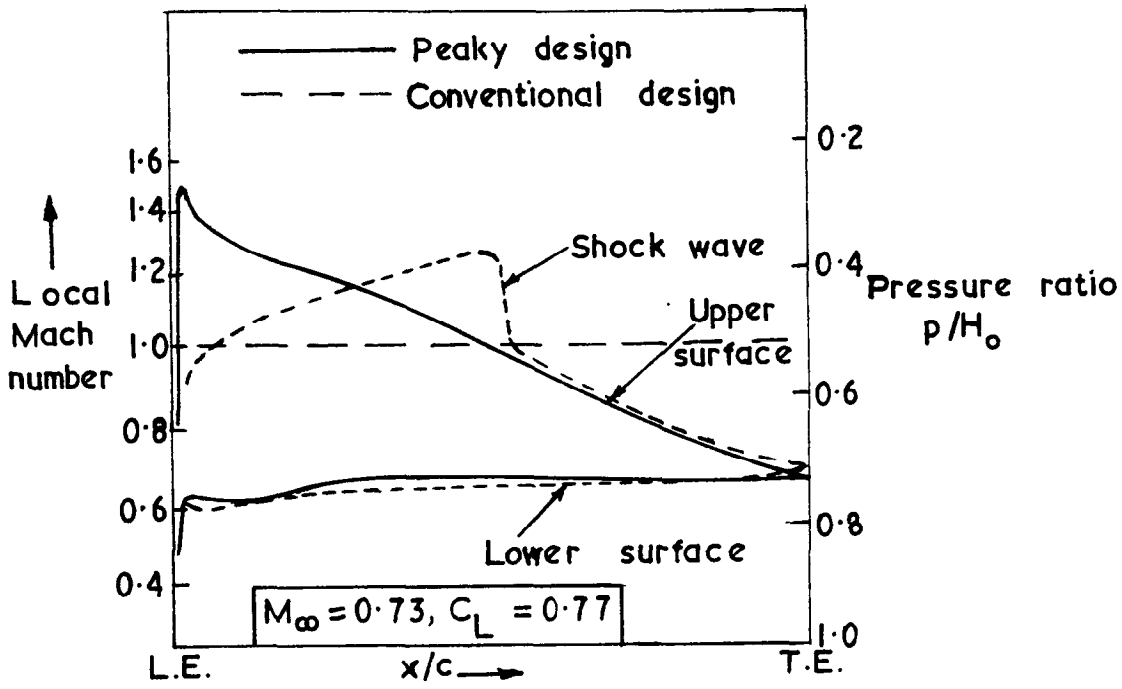

NPL 9283: Max. thickness = 8% chord

Sketch (a)

More/

More recently, alternative improvements in aerofoil performance have been realised by increasing substantially the amount of load carried over the rear half of the aerofoil, without appreciably altering the high velocities over the forward part of the upper surface. (Sketch (b))

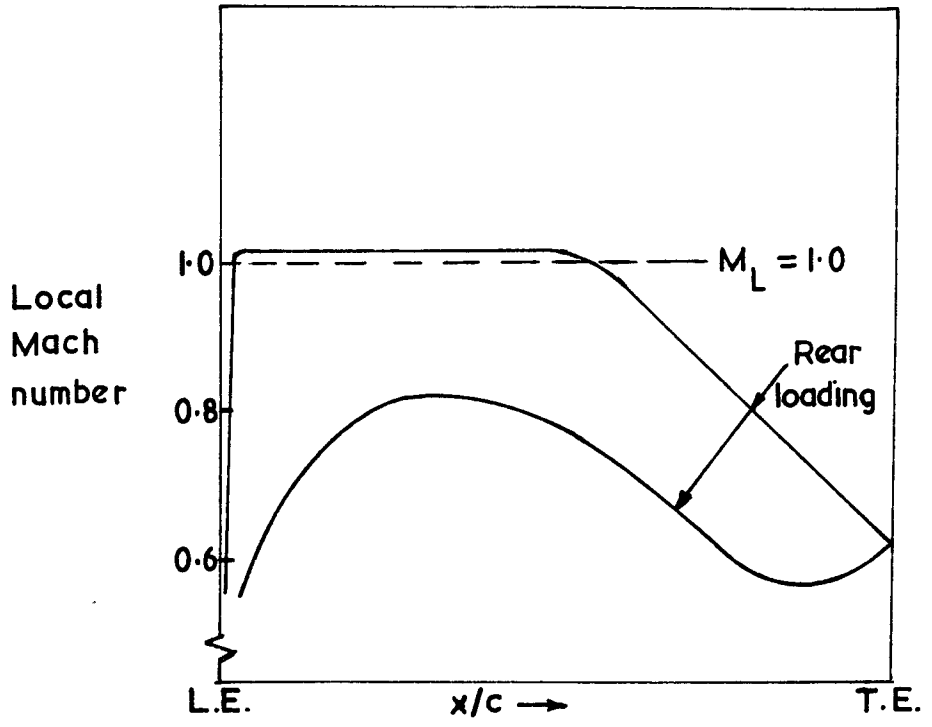

Sketch (b)

It/

It therefore seemed a natural further step to try to combine these two features in one design, and at the same time to see how far it was possible to go in extending the local supersonic region to cover a larger fraction of the upper surface than had hitherto been attempted.

The velocity distribution that was envisaged is sketched below (Sketch (c))

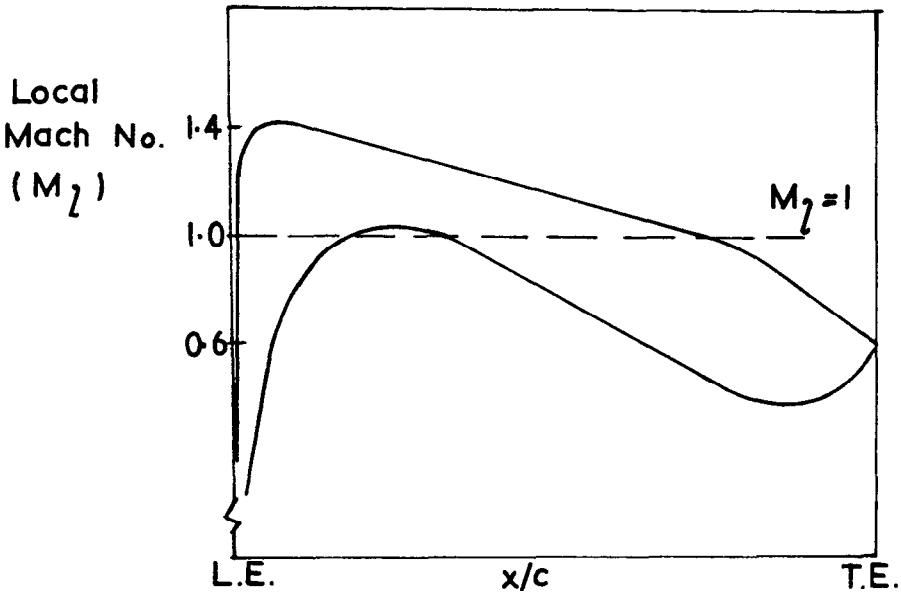

Sketch (c)

On the upper surface the velocity decreases linearly from the leading edge ($M_\ell \simeq 1.4$) to a sonic point at $x/c \simeq 0.7$ followed by a more rapid compression to the trailing edge*. On the lower surface the maximum velocity should be near sonic at $x/c \simeq 0.4$, and this is followed by a linear compression to the low velocity (high pressure) over the rear quarter chord, required to give the desired rear loading. The two design features can thus be seen to be compatible in principle; it remains to achieve them in practice.

2./

---

* It was expected at first that some form of boundary layer control would be required to suppress a rear separation, but in practice this proved to be unnecessary (at and near the design condition), and the present paper is concerned only with the results without b.l.c.

2. Design principles

In spite of the impressive advances made over the last few years by Nieuwland[2] and his colleagues, there is still no rigorous theoretical method available for general design purposes involving a substantial amount of supersonic flow; and this was even more true four years ago when the present work was started. It was therefore necessary to have recourse to an empirical approach, based principally on experience and analysis of the geometric shape of 'peaky' aerofoils which had been successful in the past (see for example Ref. 3), but coupled also with the use where appropriate of the approximate theoretical methods that were available at that time (e.g., Ref. 4) for (strictly) subcritical flows. To be more precise, the following procedure was adopted. First, the pressure distribution over the upper surface of NPL 9283 (cf. Sketch (a) above) was calculated by 'subcritical' theory at its optimum free stream Mach number ($M_\infty = 0.72$); see Sketch (d)

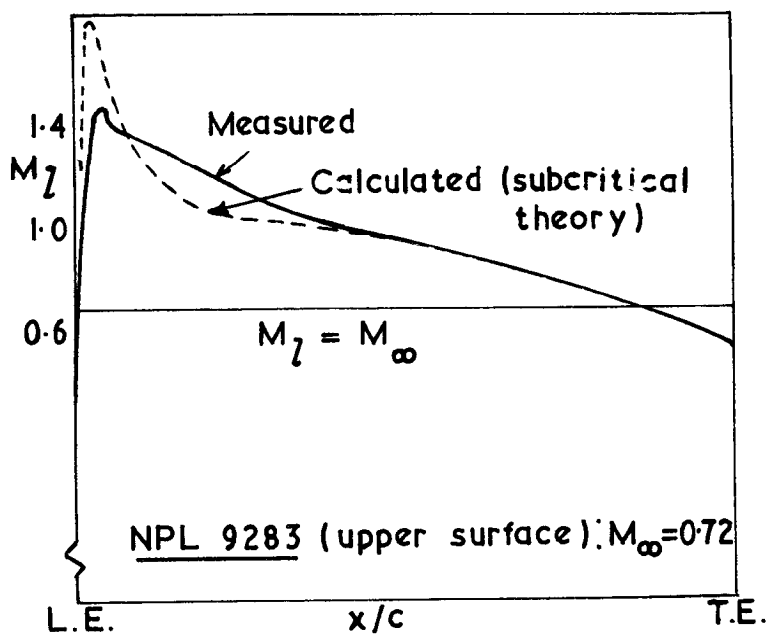

Sketch (d)

After/

After converting the calculated pressure coefficients (C_p) to local Mach number (M_ℓ), the same distribution of M_ℓ was assumed for the new section at its higher design Mach number (originally conceived as $M_\infty = 0.75$ with lift coefficient about 0.6*). but 'stretched' to cover the first 70% chord (as opposed to 40% for NPL 9283); the remaining (subsonic) part of the pressure distribution was then chosen in accordance with Sketch (c) above: see Sketch (e)

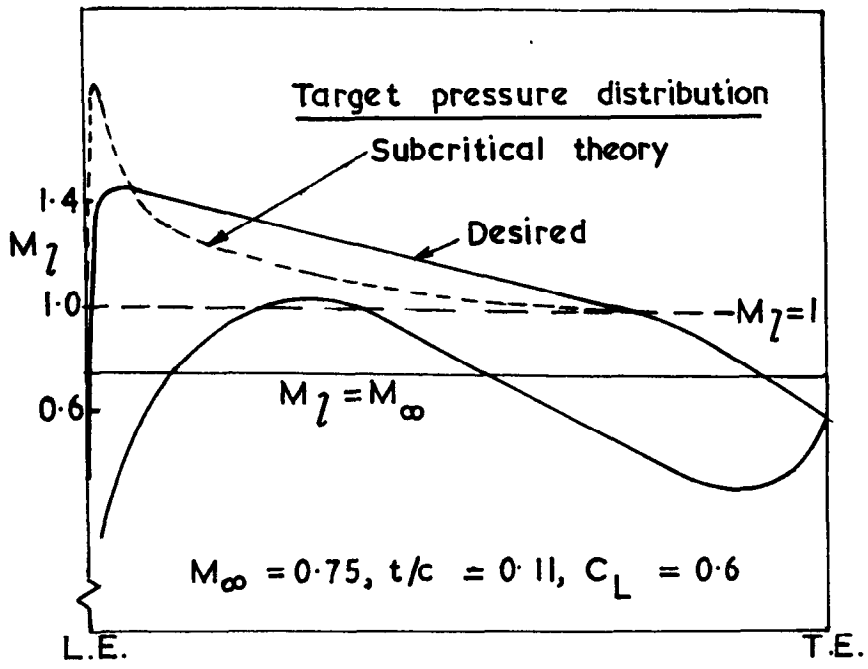

Sketch (e)

After conversion back to C_p (at $M_\infty = 0.75$), inverse techniques for the approximate theory were used to design the section shape required to produce the required 'theoretical' pressure distribution. Having done this, the curvature distribution over the forward part of the upper surface was critically examined, and adjusted to conform to the desirable criteria

established/

---

* Note however that (as described later) the optimum Mach number for the section turned out to be near 0.79; this only serves to emphasise the crudity of the design method.

established from experience (cf. Ref. 3), with a constant curvature behind the leading edge stagnation point (implying a circular leading edge) followed by a rapid reduction to as low a value as possible (consistent with the overall section geometry) over the remainder of the anticipated supersonic region: see Sketch (f)

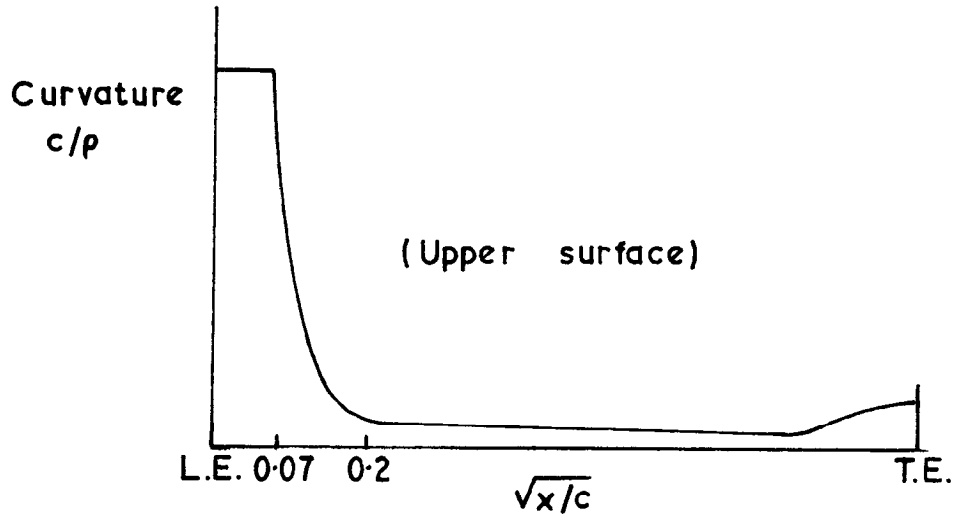

Sketch (f)

A further test was made by examining the hollowness of the leading edge 'suction loop' for incompressible flow and applying the criterion given in Ref. 5 (Section 4.2.1) for separating the 'triangular' and 'peaky' types of aerofoil; this suggested an additional minor modification to the leading edge shape. Finally, in order to alleviate the strong adverse pressure gradient over the upper surface of the aerofoil just ahead of the trailing edge, some additional thickness was added there, leaving a blunt base to the section. The thickness of this base was 0.5% of the chord, well below the expected boundary layer thickness at the trailing edge, and previous research (Ref. 6) had suggested that no appreciable drag increment would be produced by this device (which has also obvious structural advantages).

3. Details of the section and experiments

A drawing of the section (NPL 9510) is shown in Fig. 1, and details of the curvatures around the nose, and of the upper surface slopes, are shown in Fig. 2. The maximum thickness is just over 11% of chord, and the nose radius is 2% of chord. There is a blunt base of 0.5% thickness.

A 10 inch (25.4cm) chord model of the section was tested in the NPL 36 inch (91.5cm) by 14 inch (35.5cm) transonic tunnel (the effective height of this tunnel with slotted walls fitted is 30 inches (76.1cm)). The slotted walls were arranged with an open area ratio of 0.033, and were parallel.

This/

This wall condition was known to be approximately interference free over the Mach number range of interest from the results of previous experiments. Since the tunnel always has approximately atmospheric stagnation pressure, the Reynolds number varies with free stream Mach number (M_∞), in this case from about 2.65×10^6 at $M_\infty = 0.5$ to about 3.65×10^6 at $M_\infty = 0.8$, based upon model chord.

Transition tripping bands of approximately 200 grade carborundum (i.e., particle sizes of the order of .003 inches (.0076cm)) were used on the model. Most of the tests were carried out with a band from 6-8% of chord on the lower surface, and from 4-6% on the upper surface. A few tests were carried out without the band on the upper surface.

Pressures on the model were measured at 44 static holes whose positions are marked on Fig. 1, and which were spread across the central 7 inches (17.8cm) of the model. Drags were calculated from wake traverses made one chord's length downstream of the model's trailing edge.

4. Results of the experiments and discussion

The section was tested over a range of incidence (α) from $\alpha = 0°$ to $\alpha = 4°$ and a range of free stream Mach number from $M_\infty = 0.5$ to $M_\infty = 0.85$.

The overall forces on the model from some of the measurements are shown in Figs. 3 to 9 and cover the whole range of the experiments. Each figure shows the variation of the forces with free stream Mach number for a particular value of the incidence. The optimum operating conditions in terms of L/D and drag rise Mach number occurred at values of incidence of 1.75° and 2.0°, and these results will be considered first.

The most significant feature of the results at both of these incidences is the variation of drag coefficient with Mach number, which is a little unusual. The drag coefficient shows a steady upward creep with increases in free stream Mach number until just before the rapid drag rise when there is a local rather more rapid increase, followed immediately by an even more rapid decrease of significant magnitude, and then by the rapid drag rise. The lift coefficient increases steadily with increases in free stream Mach number to a maximum around the Mach number at which rapid drag rise occurs (M_D). The plots of trailing edge pressure at the top of each figure indicate that trailing edge separation is starting to occur on the upper surface just before the rapid drag rise. The value of drag rise Mach number (about 0.79) is commendably high when compared with a conventional rooftop-type section with the same lift and thickness, for which a value of M_D of about 0.71 would be expected. Also included in the figure for $\alpha = 2°$ are estimates of the boundary layer drag only, calculated using the method of Nash and Macdonald[7]. The relatively small variation of the boundary layer drag compared with the total measured values indicates that practically all of the drag creep must be attributed to the development of shock waves on the model.

Fig. 10 shows pressure distributions on the section for three Mach numbers at $\alpha = 1.75°$. At this incidence the leading edge peak on the upper surface becomes supersonic at $M_\infty = 0.55$ and the peak Mach number increases steadily to a value of about 1.38 at $M_\infty = 0.7$. With further increases in M_∞ the velocities at the peak and on the following supersonic flow on the upper surface virtually 'freeze' until well beyond rapid drag rise, and the main

effect/

effect of increasing M_∞ is on the movement of the principal shock on the upper surface. The pressure distribution in Fig. 10 for $M_\infty = 0.75$ shows a result typical for a free stream Mach number below that for rapid drag rise. Following the peak there is an isentropic recompression of the flow which ends in a normal shock. With increasing values of M_∞ the region of supersonic flow extends progressively rearward and more and more isentropic recompression occurs, with the result that the terminating shock becomes steadily weaker. The pressure distribution for $M_\infty = 0.8$ in Fig. 10 is for conditions at the bottom of the drag 'bucket' just before the final rapid drag rise. The region of supersonic flow extends slightly past the end of the low-curvature part of the upper surface at $x/c = 0.65$ and there is an almost continuous, though erratic, isentropic recompression to the terminating shock which is quite weak. By this stage the section is operating above its original design Mach number, even though this is an optimum condition, and a region of supersonic flow has also developed on the lower surface and has a terminating shock of significant strength. The last pressure distribution is for a free stream Mach number of 0.825, well above the rapid drag rise Mach number. The shock on the upper surface has moved only a small amount further downstream but has increased significantly in strength; the shock on the lower surface has also become much stronger. This 'sticking' of the upper surface shock at about 70% of chord, where the surface curvature changes, always occurred, and even strong shocks causing total boundary layer separation downstream did not move far from this point.

Fig. 11 shows schlieren photographs corresponding to the three pressure distributions in Fig. 10. The two shocks coming from upper surface leading edge of the model are from the front and rear of the carborundum band; they were, in fact, quite weak and caused only minor perturbations in the pressure distribution. The photograph for $M_\infty = 0.75$ shows a sharply defined shock of limited extent on the upper surface of the aerofoil at the end of the region of supersonic flow. At other free stream Mach numbers below the optimum the appearance of the shock was similar to that in this photograph except that it extended steadily to greater distances above the model as it moved downstream. At $M_\infty = 0.8$ (the optimum Mach number) the pattern of the terminating shock is confused (partly because there appeared to be some variation in the position of this shock across the model) and, although it extends for a considerable distance (about 75% of model chord), gives the appearance of dissipating rapidly above the model. This apparent weakness of the shock out in the stream was confirmed by the pitot traverses made in the wake, the measured momentum deficit being very small over large distances in this region. The photograph for $M_\infty = 0.825$ shows that the terminating shock on the upper surface has moved very little, but appears to have strengthened considerably, and has caused total separation of the boundary layer. This was again confirmed by the wake traverse, which recorded a marked momentum deficit well out into the stream. The latter two photographs also show the development of the shock on the lower surface, and at the highest Mach number this shock has caused total separation of the lower surface boundary layer.

The rapid variations in drag just before the rapid drag rise can now be explained in terms of the shock development on the upper surface of the model. Since the drag due to a shock will depend upon both its strength and its extent in the free stream, the occurrence in this case of a shock whose strength decreases as its extent increases leads to the possibility of its drag either increasing or decreasing as it develops. At the lower free

stream/

stream Mach numbers the rate of extension of the shock must outweigh the rate at which its strength is decreasing and cause a net increase in drag which produces most of the pronounced drag creep observable in the results. A stage is eventually reached, however, when the rate of reduction of the shock strength outweighs its rate of extension and a net reduction in shock drag occurs, as is also observed in the results.

Fig. 12 shows three pressure distributions for $\alpha = 2°$; these display quite similar characteristics to those at 1.75°. The shock development on the upper surface was also similar to that shown in Fig. 10.

The suddenness at which the drag falls just before drag rise can be explained by the very rapid movement of the terminating shock at these free stream Mach numbers. Fig. 13 is a plot of the shock position against M_∞ for $\alpha = 1.75°$ and $\alpha = 2°$. In both cases the shock moves about 40% of chord from the free stream Mach number just ahead of the drag 'hump' to that at the minimum, this being for a change in M_∞ of about 0.03. Since the strength of this shock will depend upon its position rather than the free stream Mach number, a rapid change in drag with M_∞ can be understood readily.

The final upward turn just before the drag falls off rapidly is apparently associated with the principal upper surface shock passing the crest. Fig. 14 shows a plot of the free stream Mach number at which this occurs at various incidences together with a plot of the free stream Mach number for which the shock is at the crest, and there appears to be a correlation between these two occurrences. Such a result cannot be considered general for this sort of aerofoil, however, since the shock development is so much more complex than for the usual section to which this criterion is confidently applied. It seems likely that for a slightly different section form the balance between the shock's strength and extent could quite easily have been producing a decrease in shock drag as it passed over the crest sufficient to eliminate the effect entirely.

The pressure distributions in Figs. 10 and 12 show that, for this aerofoil section, most of the lift is being produced by the supersonic flow on the upper surface and by the rear loading. Without these features the available lift would be of little consequence. It is of interest that two features which have usually been regarded as methods of improving a section's performance, rather than as the principal contributors to its load-carrying ability, are here doing almost all of the work, and to the extent of producing a lift coefficient of very respectable order together with a value of drag rise Mach number well beyond that which could be expected from normal methods.

It is useful to know how the amount of isentropic recompression obtained on the upper surface compares with what is theoretically possible. This is best done using a characteristic diagram with the parameters θ (surface slope), $\theta + \omega$, and $\theta_8 - \omega$ (ω being the Prandtl-Meyer function) in the manner described by Pearcey[8]. Such a diagram for a typical result is shown in Fig. 15 for $M_\infty = 0.785$ and $\alpha = 2°$. The work of Moulden[9] predicted that the maximum theoretical rate of compression that is permissible results in the curve for $\theta - \omega$ being horizontal on this plot. If the slope of this curve becomes negative it implies that the compression waves in the flow are crossing over one another and a shock should result. The figure thus shows that over most of the low curvature part of the surface the recompression rate is the maximum possible. This figure also indicates which part of the expansion from the

peak/

peak 'reflects' back from the sonic line onto the aerofoil as compression. A horizontal line from a point at some x/c value on the $\theta - \omega$ curve, cuts the $\theta + \omega$ curve at the point where expansion from the first point reflects back onto the surface as compression. The figure shows that it is expansion up to only about the first 4% of chord that affects the downstream recompression rate.

There was some concern that, because of the closeness of the recompression rate to the maximum possible, the disturbance caused by the double shock from the carborundum band, weak though it was, might adversely affect the recompression characteristics of the flow. To check this some tests were made with the upper surface band removed. Fig. 16 shows pressure distributions for $\alpha = 2^\circ$ and $M_\infty = 0.785$ for tests both with and without the carborundum band. This case, being at an optimum condition, ought to be sensitive to any possible effects. The figure shows negligible difference in the lower surface behaviour and slight differences in the supersonic flow on the upper surface; the main effect is a slightly more rearward position of the shock. Overall forces where measured with transition free are shown on Figs. 6 and 7. The drags are a little lower and the lifts a little higher, but the essential features of the results are maintained, particularly the values of drag rise Mach number, and nothing occurs that could not be explained in terms of the thinner boundary layer resulting from the more rearward transition position. In general the upper surface supersonic recompressions of the transition free results seemed to be slightly better in quality than those with a carborundum band on the model, but there was no occurrence that in any way altered the general conclusions drawn from the results.

The pressure distributions of the supersonic flow on the upper surface showed similarities at nearly all incidences. Fig. 17 shows pressures for this region for the whole range of incidences tested at a free stream Mach number of approximately 0.775 (the precise value is not significant because of the freezing of the pressure distribution in this region). The rate of recompression is very similar for all incidences above $\alpha = 1^\circ$ and the local Mach number is thus dependent mainly on the peak Mach number, which increased with incidence. This similarity also carries over to the characteristics plot, which is shown in Fig. 18. The recompression rate at all incidences is virtually at the maximum possible.

Because of the higher overall supersonic velocities at the higher incidences of 3° and 4°, the terminating shock on the upper surfaces was stronger and immediately induced total boundary-layer separation. This combination of a stronger shock and separation seems to be the main reason for the much higher drags at these incidences which can be seen in Figs. 8 and 9. Also at $\alpha = 4^\circ$ there was total separation at the leading edge at lower free stream Mach numbers because the deceleration following the subsonic peak was much more severe than that following the supersonic peak; once the supersonic peak was established the boundary layer was always perfectly attached and well behaved until the terminating shock was reached.

At the incidences below 1.75° the occurrence of drag rise became more dependent upon the development of the lower surface shock. At drag rise at $\alpha = 0^\circ$, for example, there was no shock of significant strength on the upper surface at all, but total separation from a strong shock on the lower surface. Even at $\alpha = 1.5^\circ$, the drag rise was really governed by the development of the lower surface shock. Also at the lower incidences there was a tendency for

double/

double shocks to form on the upper surface. Though, as Fig. 17 shows, there was a leading edge peak and subsequent recompression, the terminating shock to this stayed well forward before the rapid drag rise and a second supersonic acceleration, and subsequent shock at about 60-70% of chord developed. An example of such a pressure distribution is shown in Fig. 19. A continuous supersonic recompression would not develop on the upper surface until free stream Mach numbers of about 0.825 and above, when drag rise had already been caused by the lower surface shock. This is probably the reason for the absence of the drag variations noted at $\alpha = 1.75^\circ$ and $\alpha = 2^\circ$ at lower incidences. By the time the flow over the upper surface had reached the condition where rapid variations in drag might occur, the drag was totally dominated by the lower surface shock strength and all other effects were swamped. If the section was drastically thinned on the lower surface to remove its shock, the effects noted at $\alpha = 1.75^\circ$ and $\alpha = 2^\circ$ would probably reappear.

5. Conclusions

The results described indicate that a wing section with a large amount of supersonic flow on the upper surface and heavy rear loading can operate quite satisfactorily, at least at its optimum condition, with a useful amount of lift, a considerable improvement in drag rise Mach number over conventional types and at a reasonable drag level. Though the section described is not immediately useful because of undesirable off-design characteristics there is some hope that these can be overcome. A tendency to early trailing edge separation (and resultant reduction of buffet boundary) should not be difficult to cure, nor is there any reason to suppose that the rather violent variations in drag occurring just before drag rise are an inevitable characteristic of sections of this sort. In fact a number of modified forms of the basic section have been tested and have all shown some improvement in this area. The most difficult problem to solve will probably be that of behaviour at high incidence and moderate Mach number where there will be a tendency for high velocity peaks and strong upper surface shocks to form; but much further work will be necessary to show how severe a limiting factor this is.

Acknowledgements

Thanks are due to Miss D. K. Cox for her assistance with the figures.

References/

References

No.	Author(s)	Title, etc.
1		National Physical Laboratory: Report for the year 1963 (p.24), H.M.S.O.
2	G. Y. Nieuwland	Transonic potential flow about a family of quasi-elliptical aerofoil sections.- NLR-TR T 172. (1967).
3	P. G. Wilby	Leading edge supersonic velocity peaks.- AGARD CP 35-14. (1968).
4		Method for predicting the pressure distribution in swept wings with subsonic attached flow.- Roy. Aero. Soc. Transonic Data Memo. 6312. (1963).
5		A method of estimating drag rise Mach number for two-dimensional aerofoil sections.- Roy. Aero. Soc. Transonic Data Memo. 6407. (1964).
6		National Physical Laboratory: Report for the year 1964 (p.21), H.M.S.O.
7	J. F. Nash and A. G. J. Macdonald	The calculation of momentum thickness in a turbulent boundary layer at Mach numbers up to unity.- NPL Aero. Report 1207. ARC CP 963. (July, 1966).
8	H. H. Pearcey	The aerodynamic design of section shapes for swept wings. Advances in Aeron. Sciences, Vols. 3-4, p.227. (1961). Pergamon Press.
9	T. H. Moulden	Some comments on the conditions in a local supersonic flow region.- A.R.C. C.P.1023. (1967).

Produced in England by Her Majesty's Stationery Office, Reprographic Centre, Basildon

PES R 74501/1/505376 K4 5/74 TP/P

Pressure tapping points marked

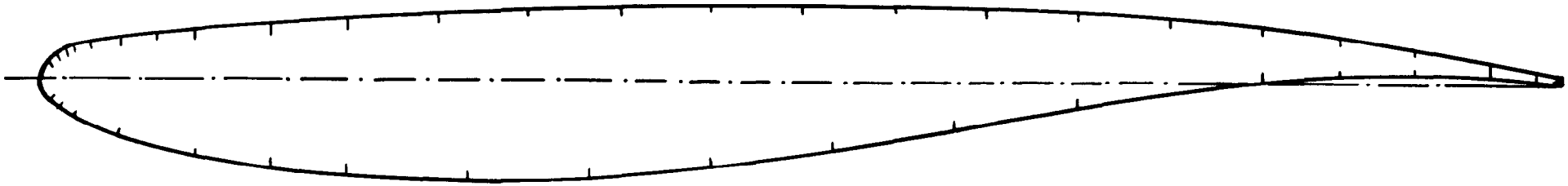

FIG. 1
31312

Aerofoil section NPL 9510

31312

FIG.2

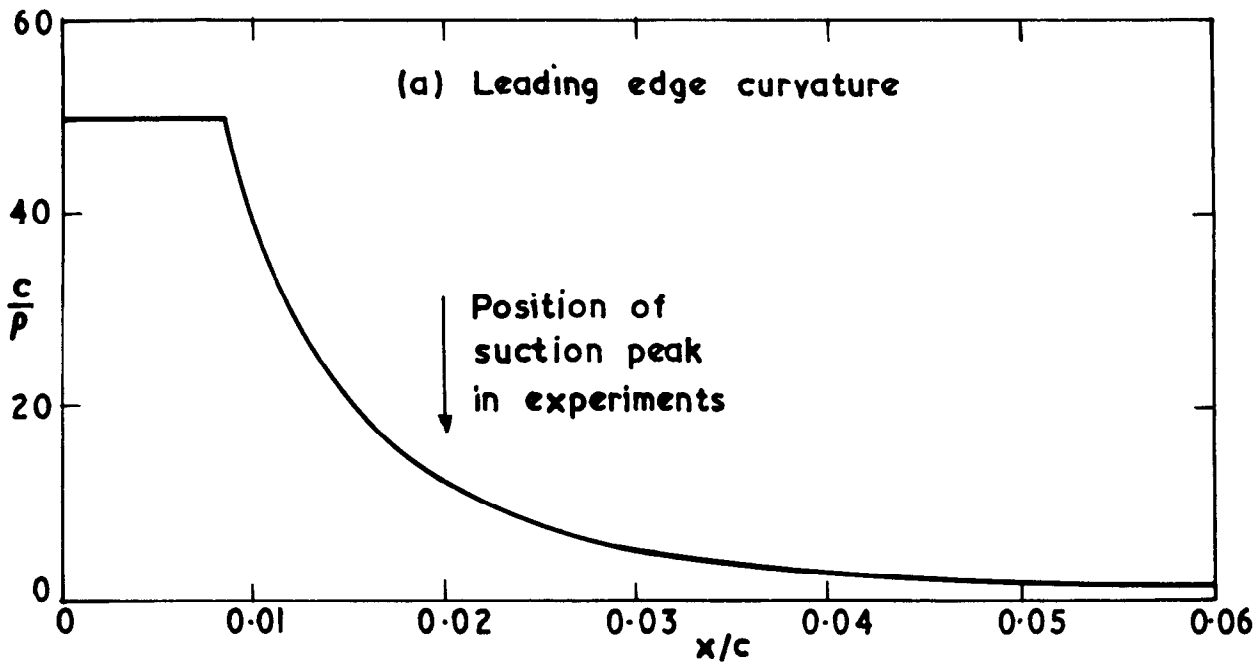

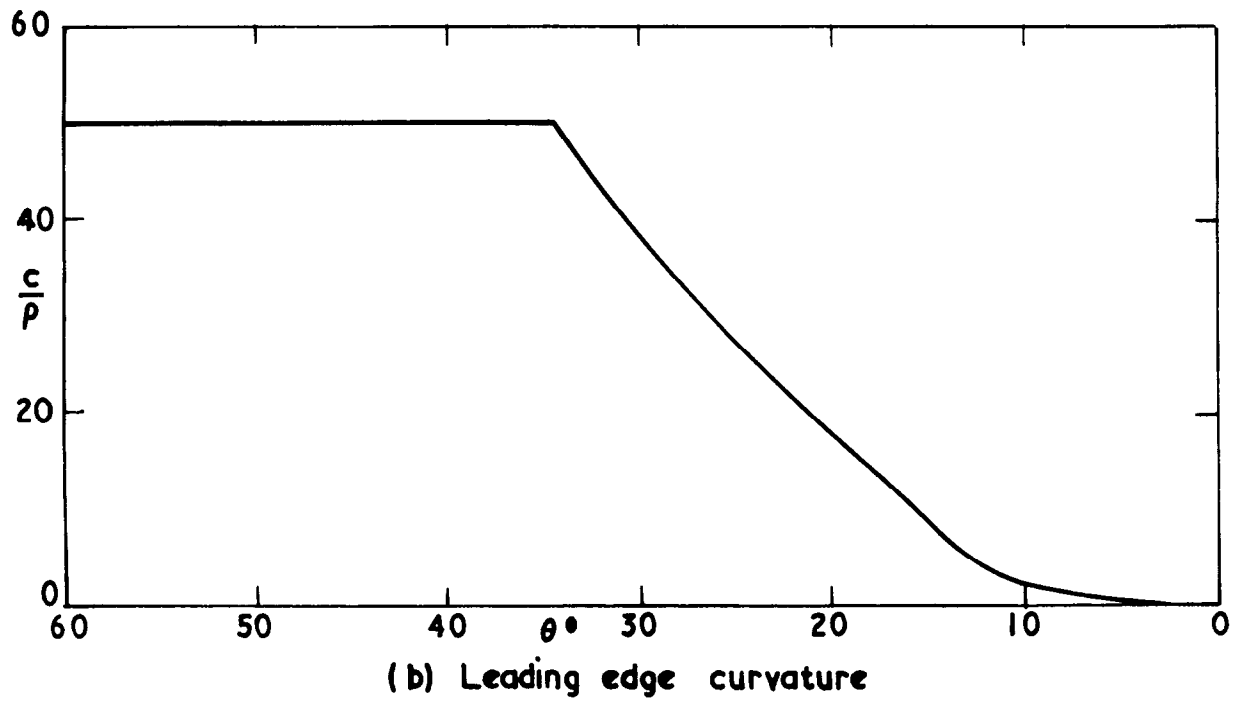

(b) Leading edge curvature

Aerofoil section NPL 9510. Details of upper surface shape

31312

FIG. 2 (cont)

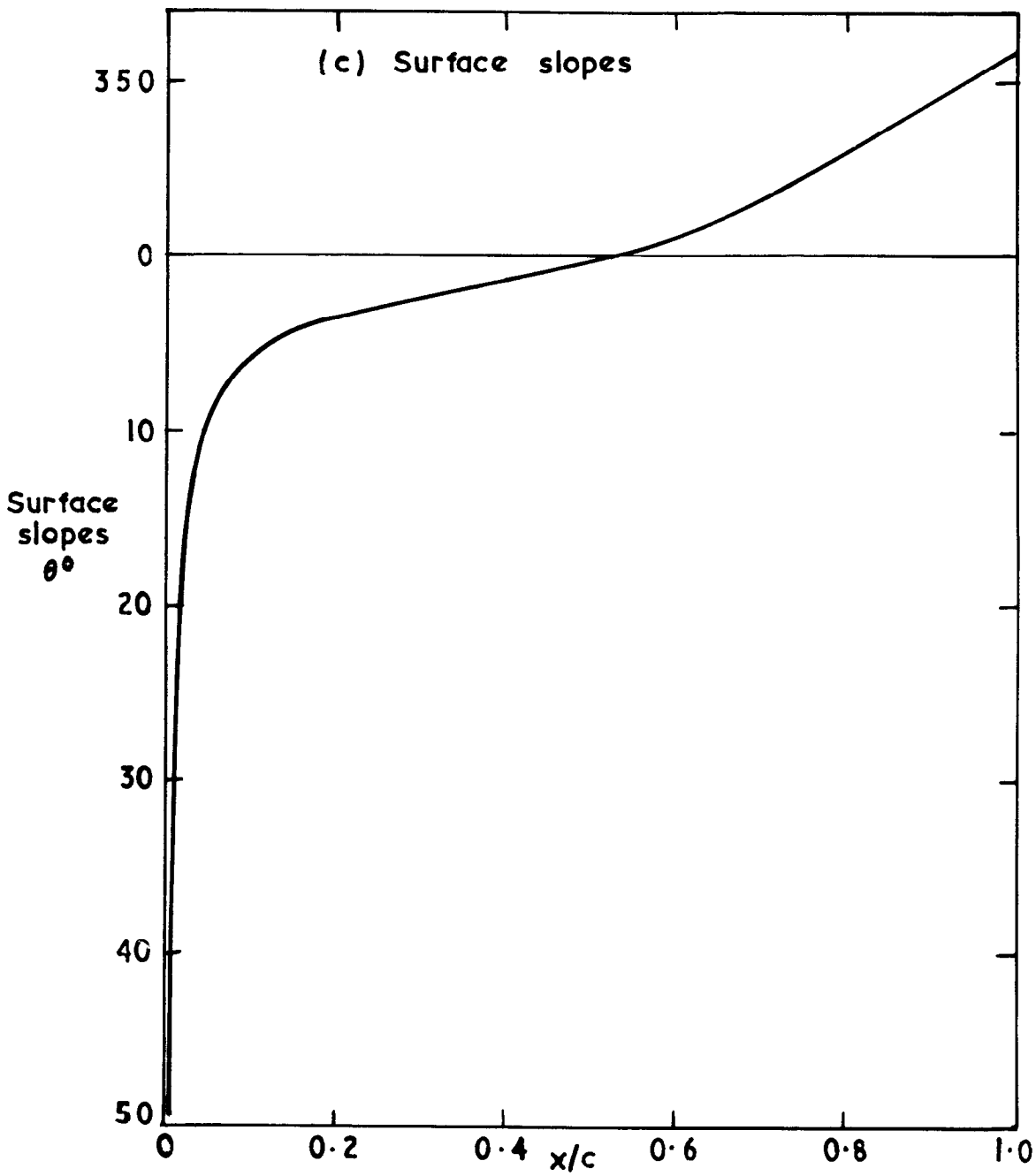

Aerofoil section NPL 9510. Details of upper surface shape.

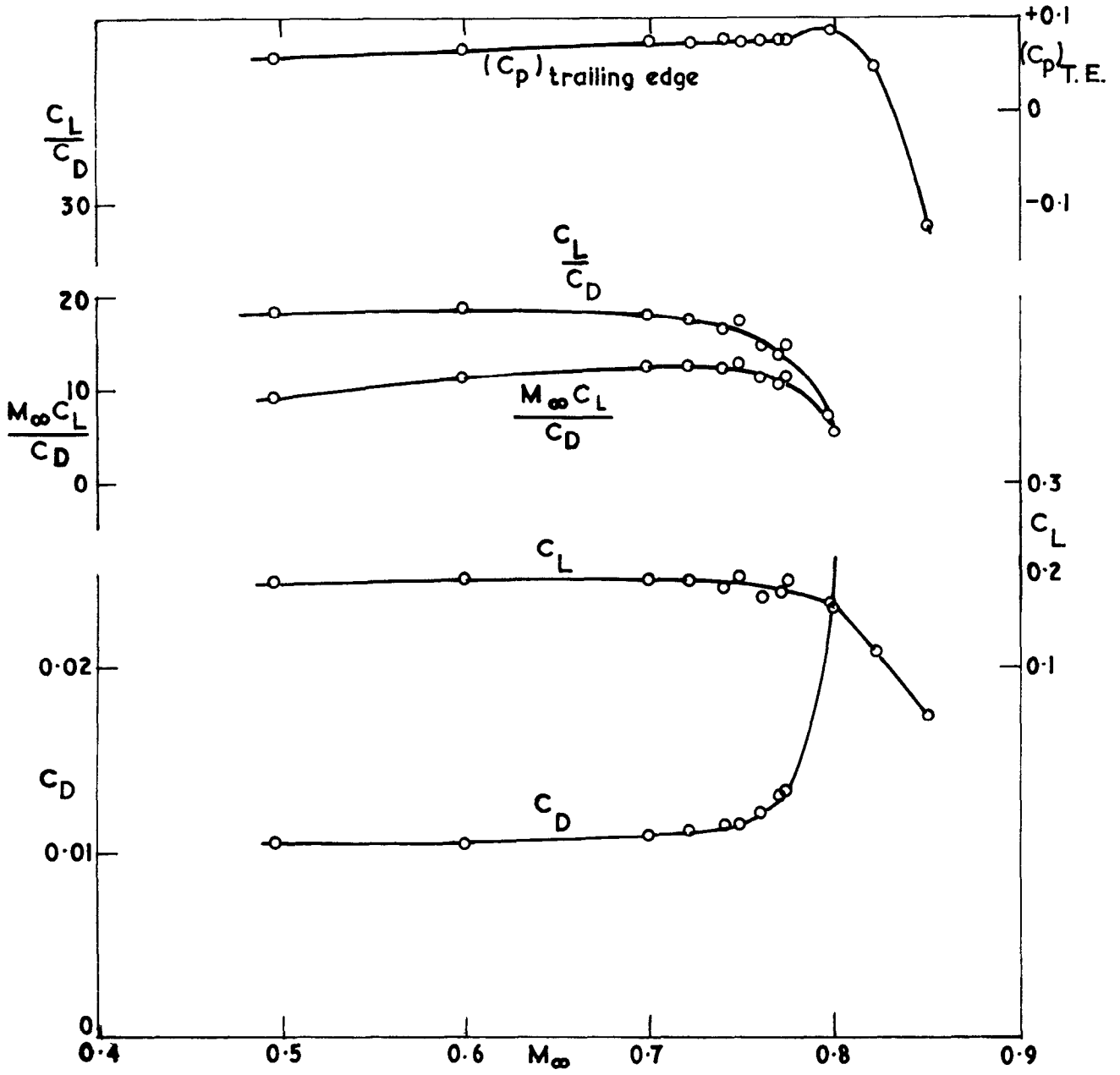

Aerofoil NPL 9510. Overall force measurements $\alpha = 0^0$

31312
FIG. 4

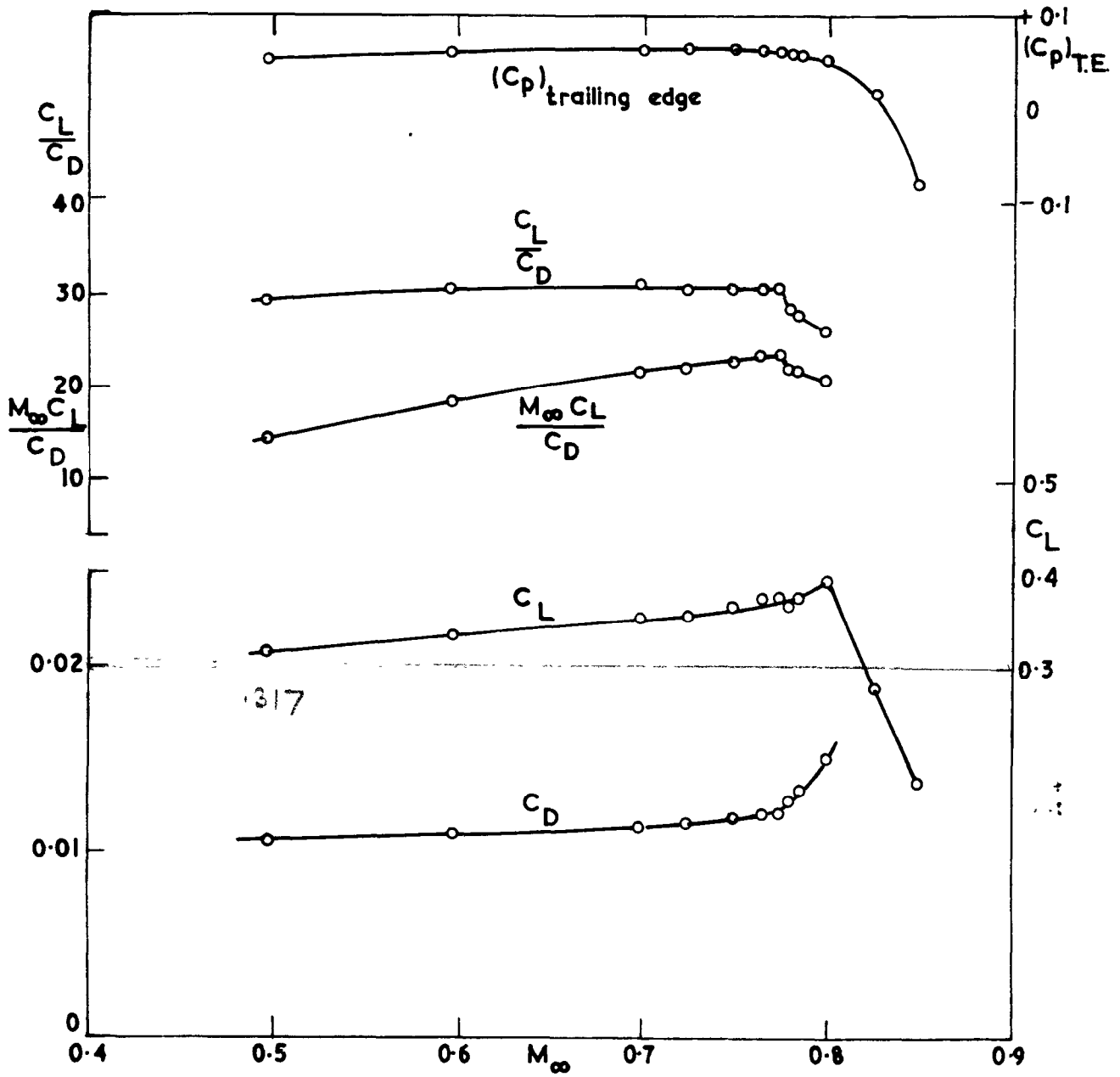

Aerofoil NPL 9510 . Overall force measurements $\alpha = 1{\cdot}0^\circ$

31312
FIG. 5

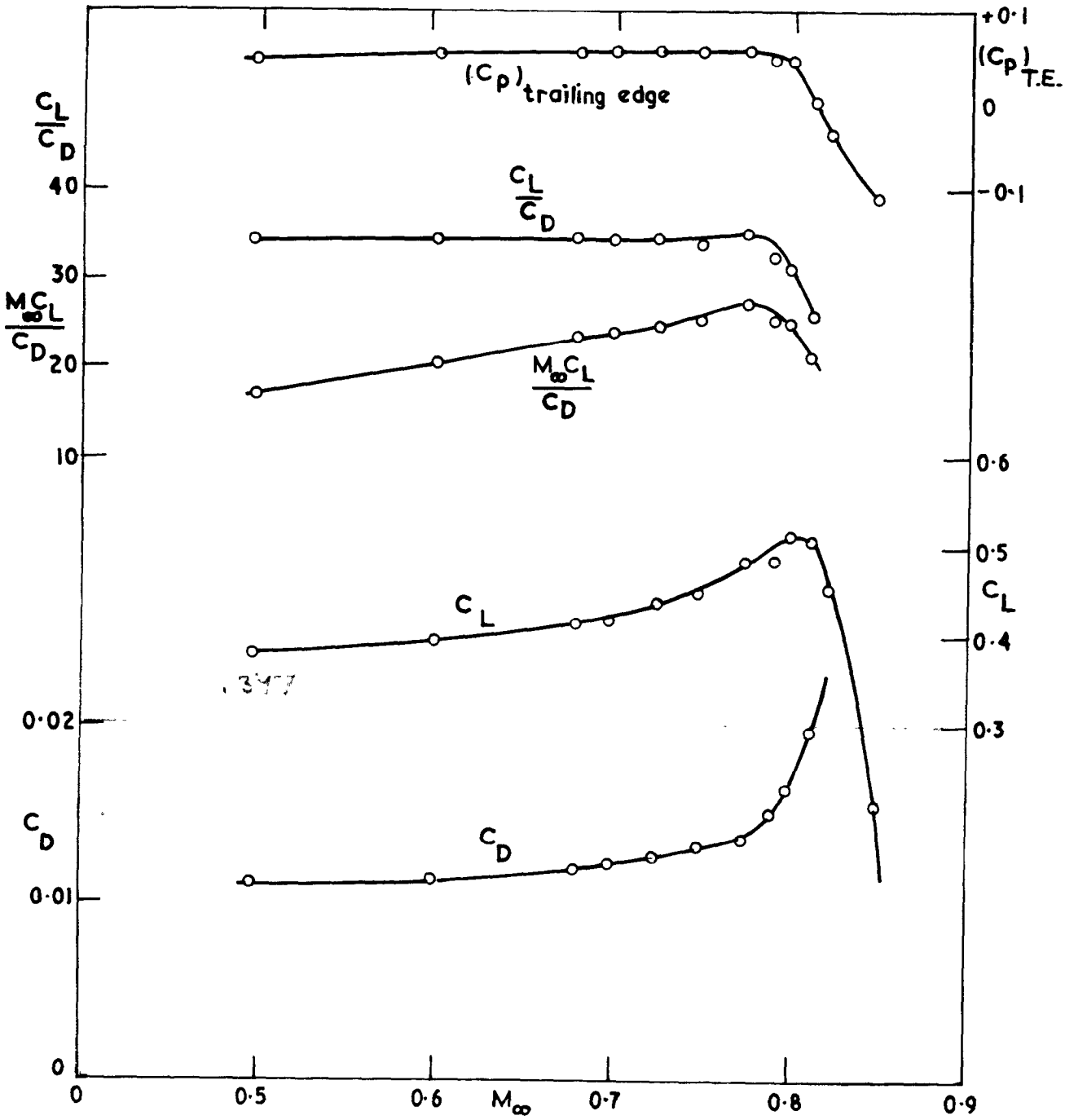

Aerofoil NPL 9510. Overall force measurements $\alpha = 1{\cdot}5°$

31312
FIG. 6

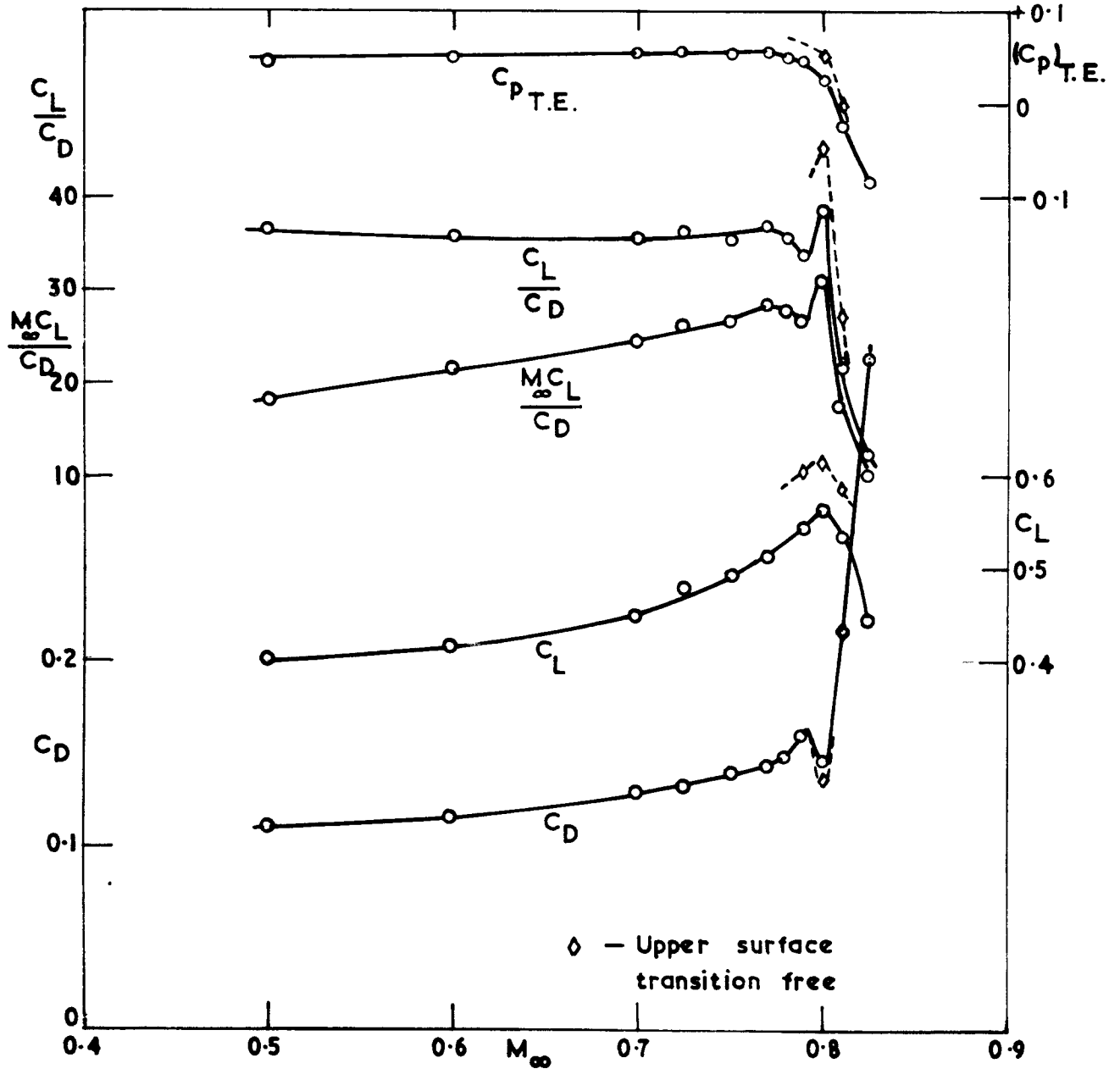

Aerofoil NPL 9510. Overall force measurements $\alpha = 1{\cdot}75^0$

31312
FIG. 7

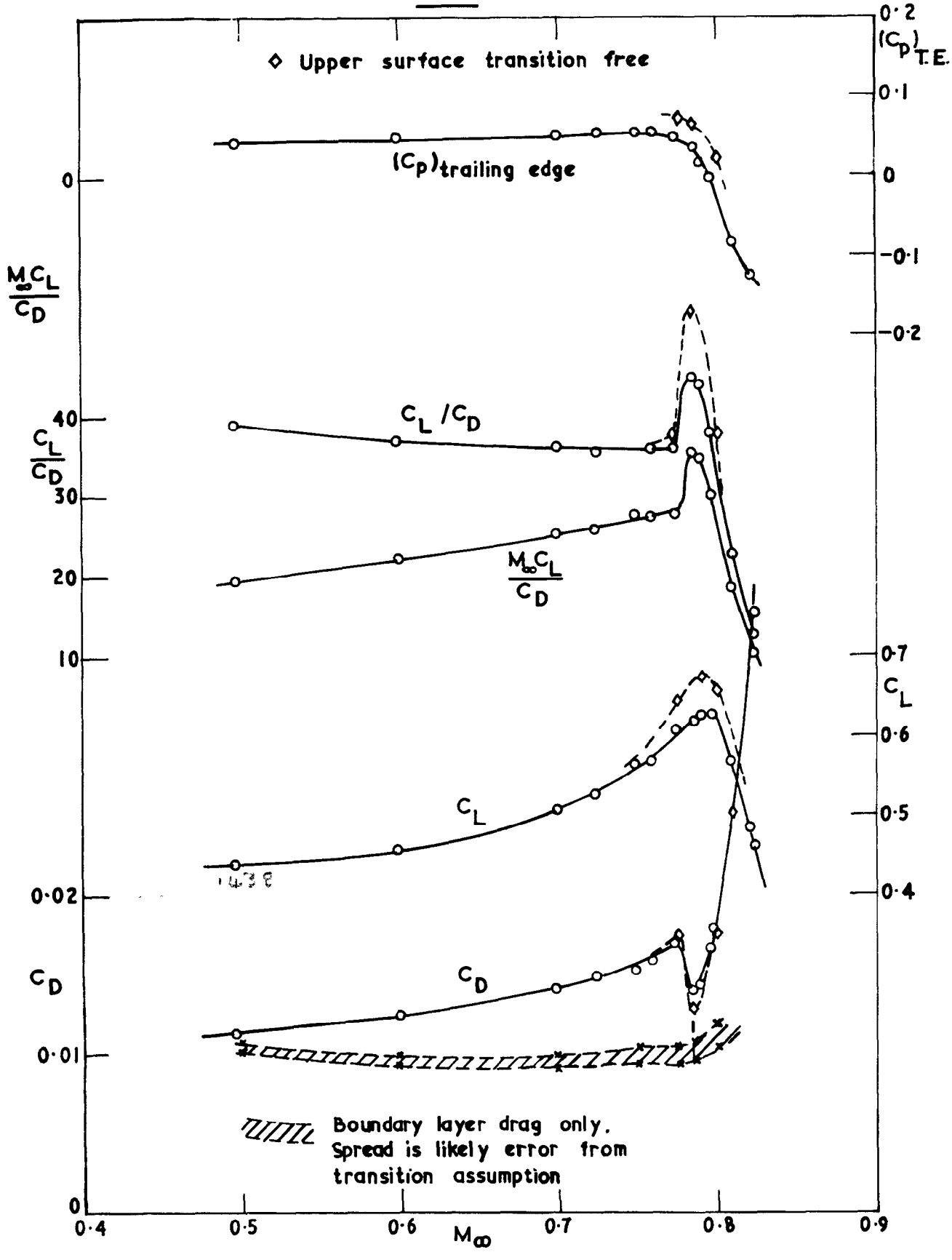

Aerofoil NPL 9510. Overall force measurements $\alpha = 2°$

31 312

FIG. 8

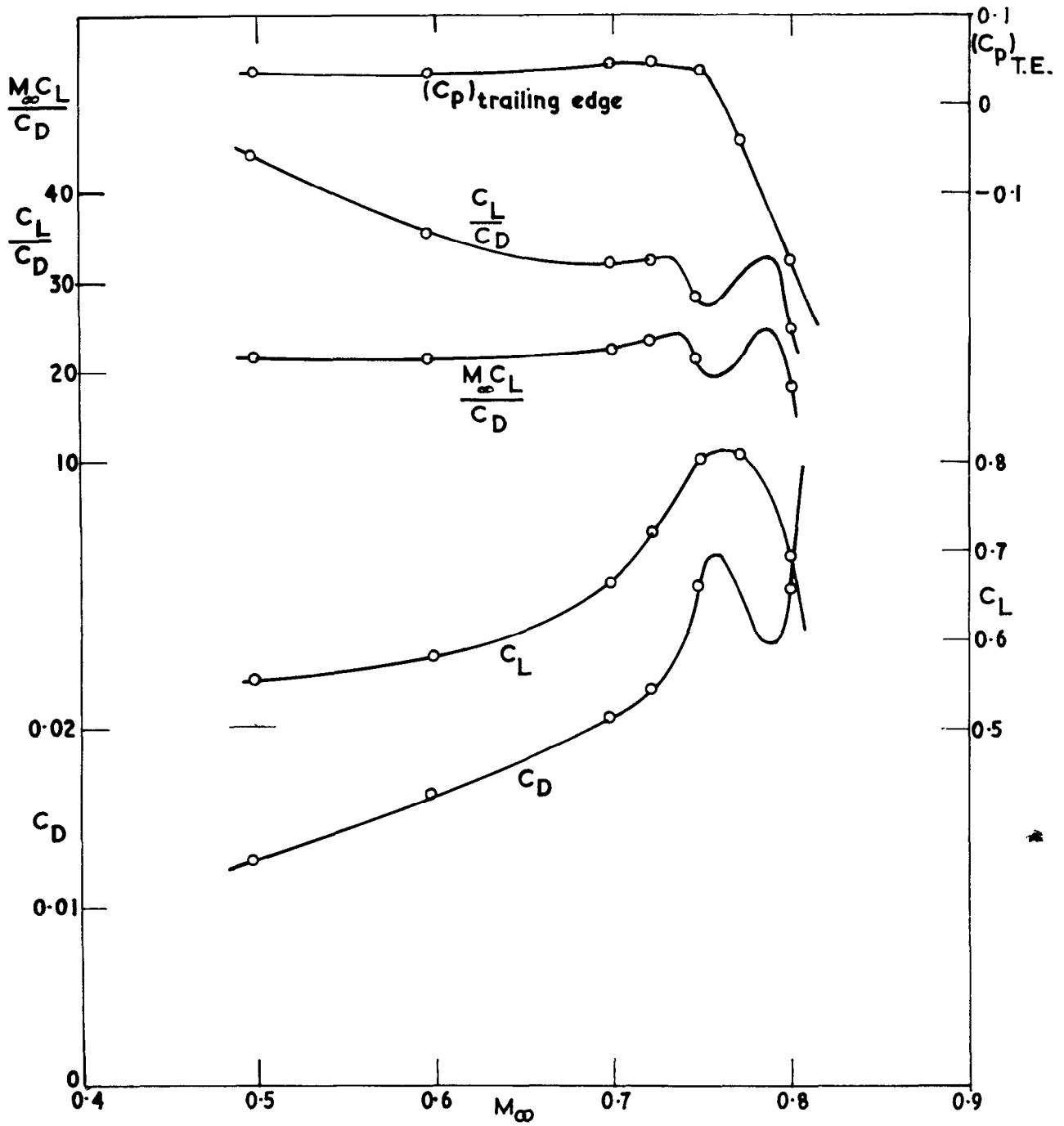

Aerofoil 9510 . Overall force measurements $\alpha = 3^\circ$

31312
FIG. 9

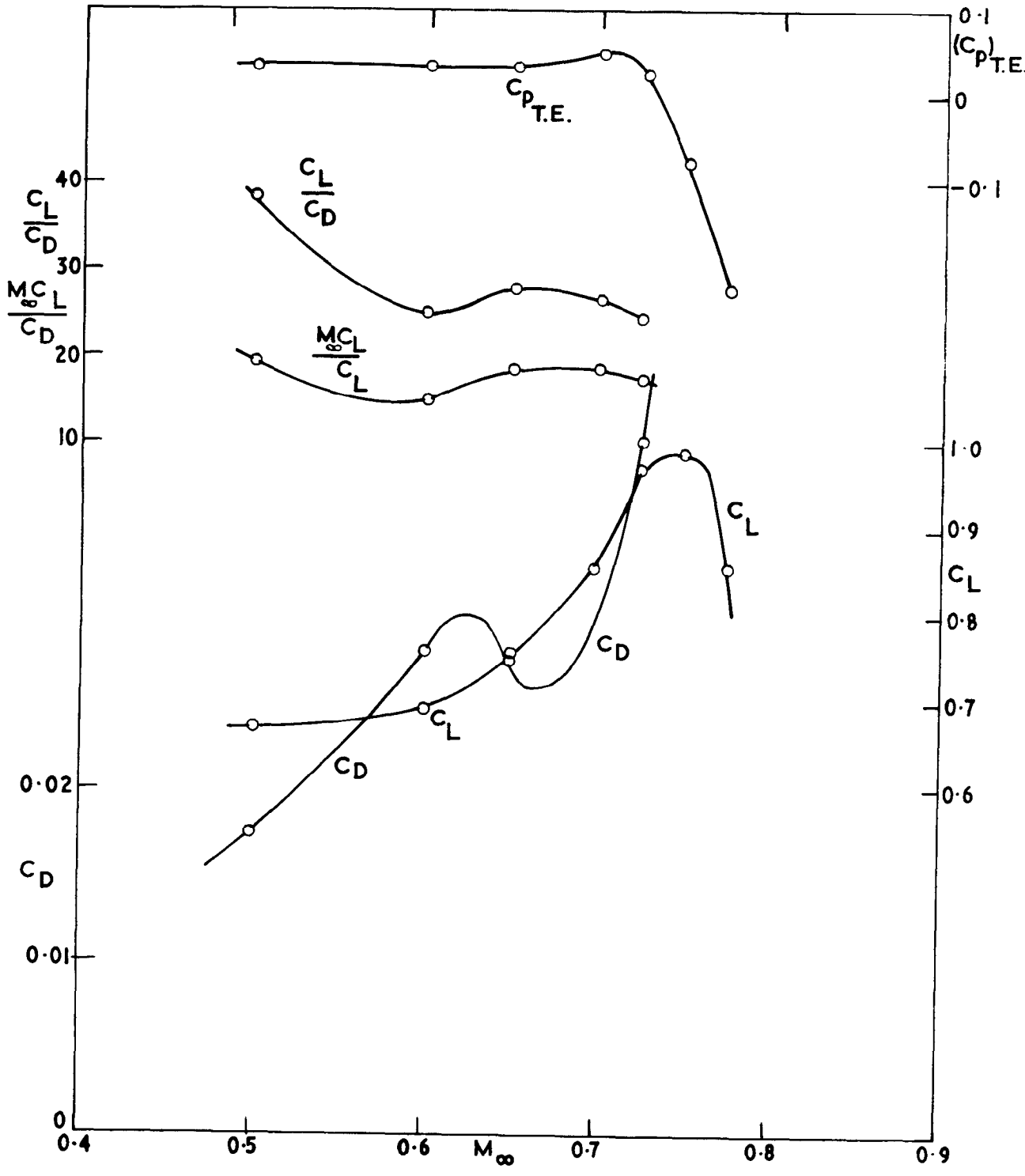

Aerofoil NPL 9510. Overall force measurements $\alpha = 4^\circ$

31 312
FIG. 10

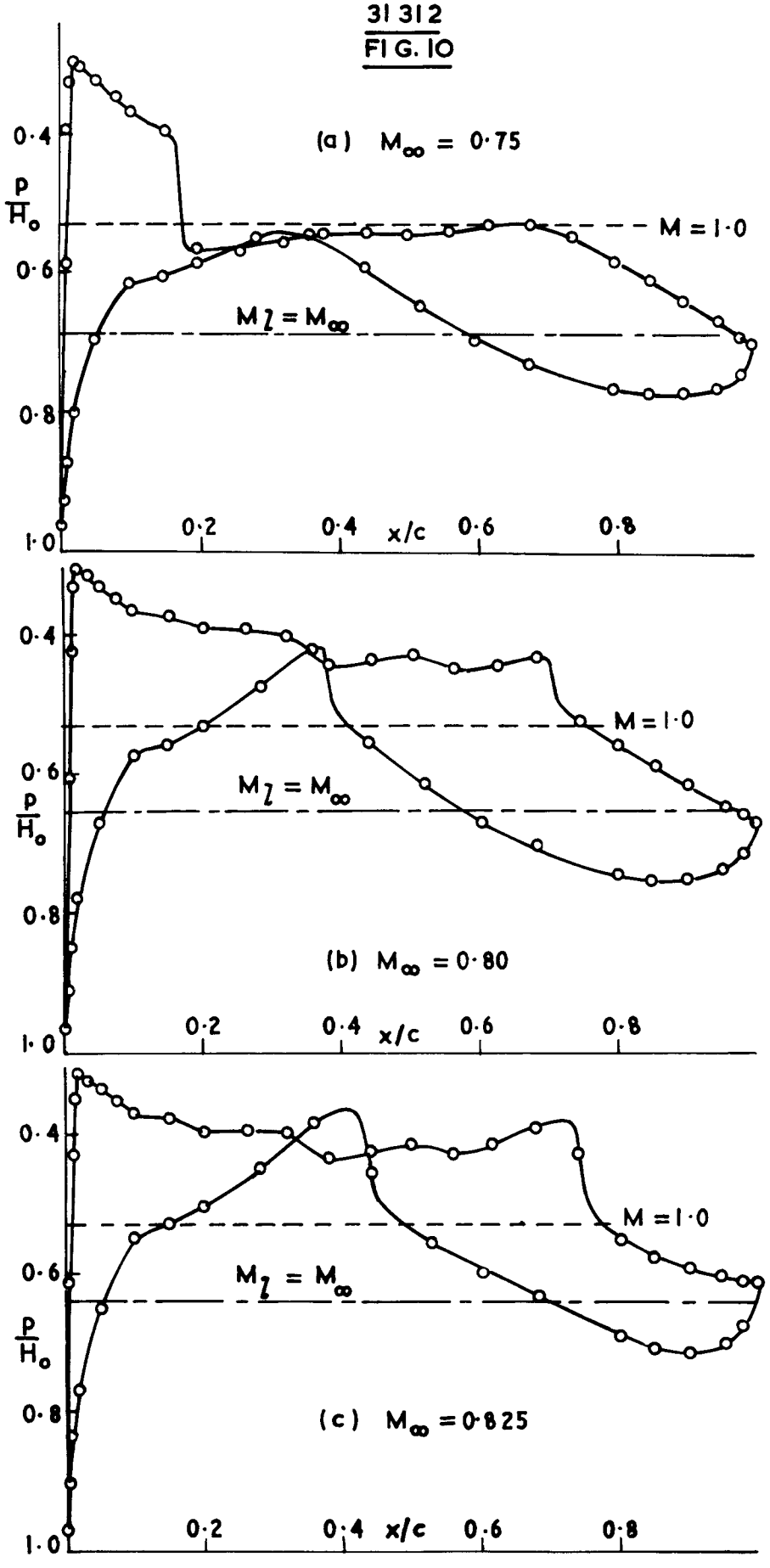

Aerofoil NPL 9510. Pressure distributions $\alpha = 1{\cdot}75^\circ$

31 312
FIG.11.

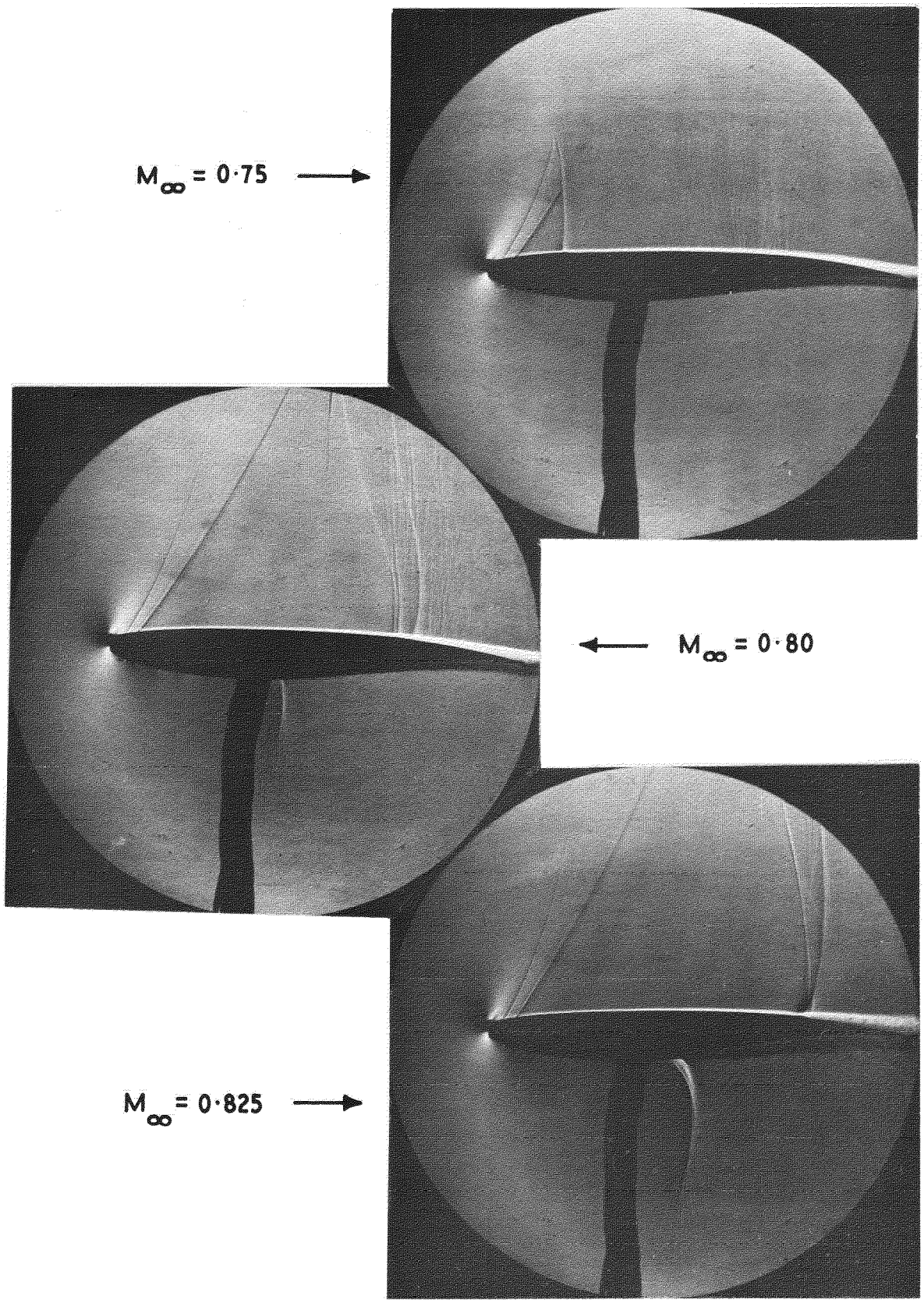

Aerofoil section NPL 9510. $\alpha = 1{\cdot}75^0$

31312
FIG.12

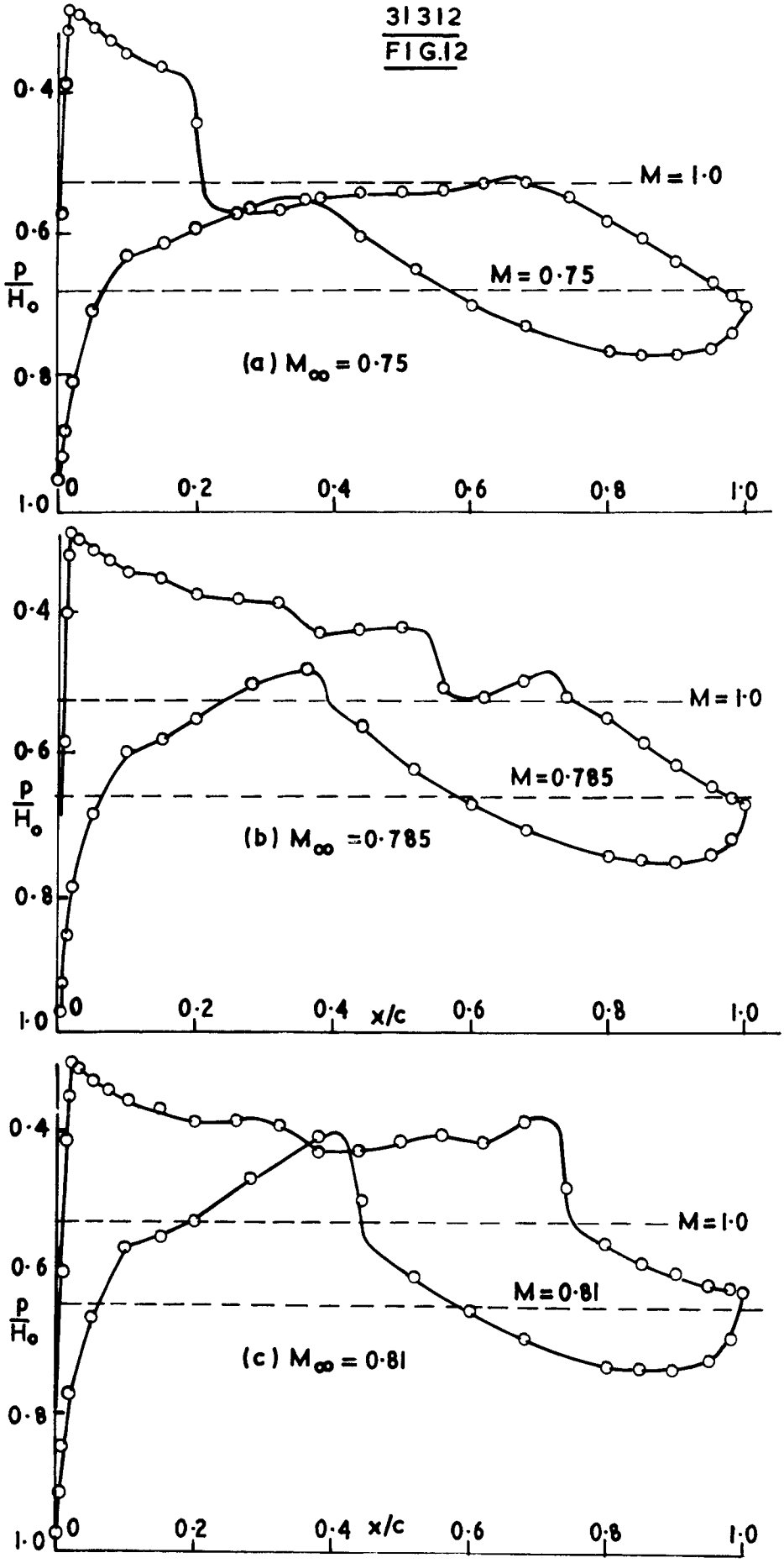

Aerofoil NPL 9510. $\alpha = 2^{\circ}$

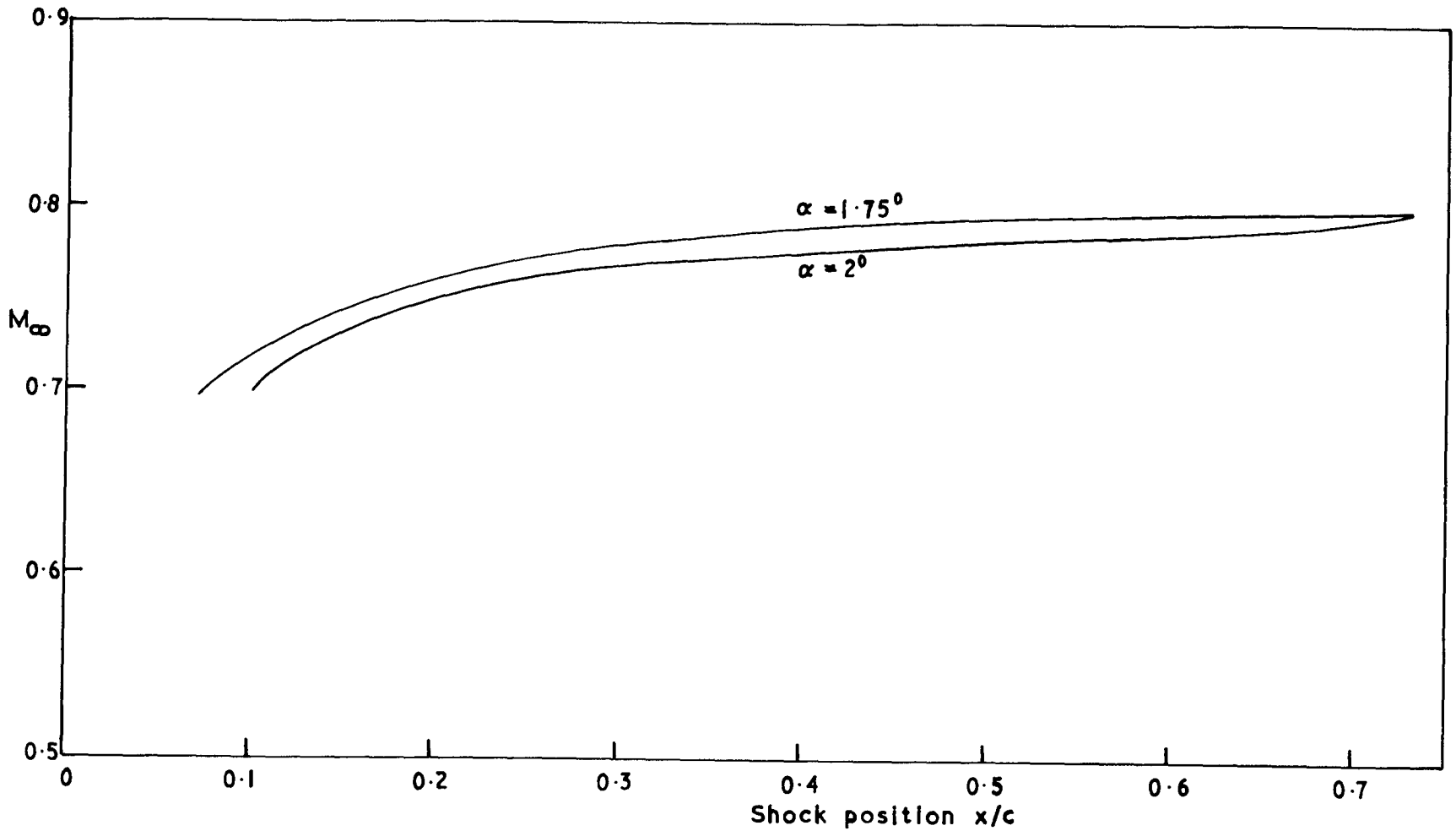

31312
FIG.13

Aerofoil section NPL 9510. Movement of principal upper surface shock.

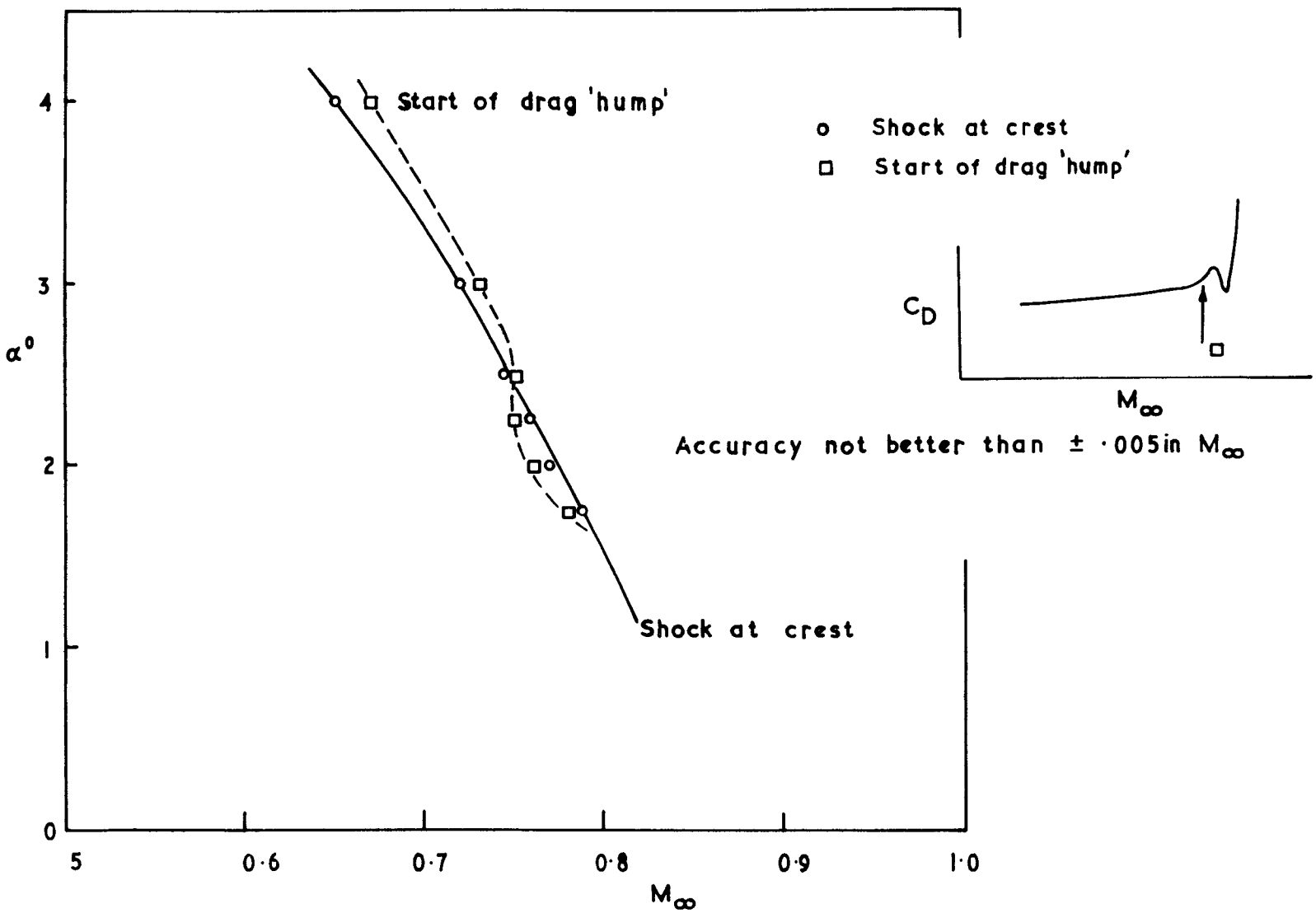

31312
FIG. 14

Aerofoil NPL 9510. Correlation between drag 'hump' and 'shock at crest'.

31312
FIG. 15

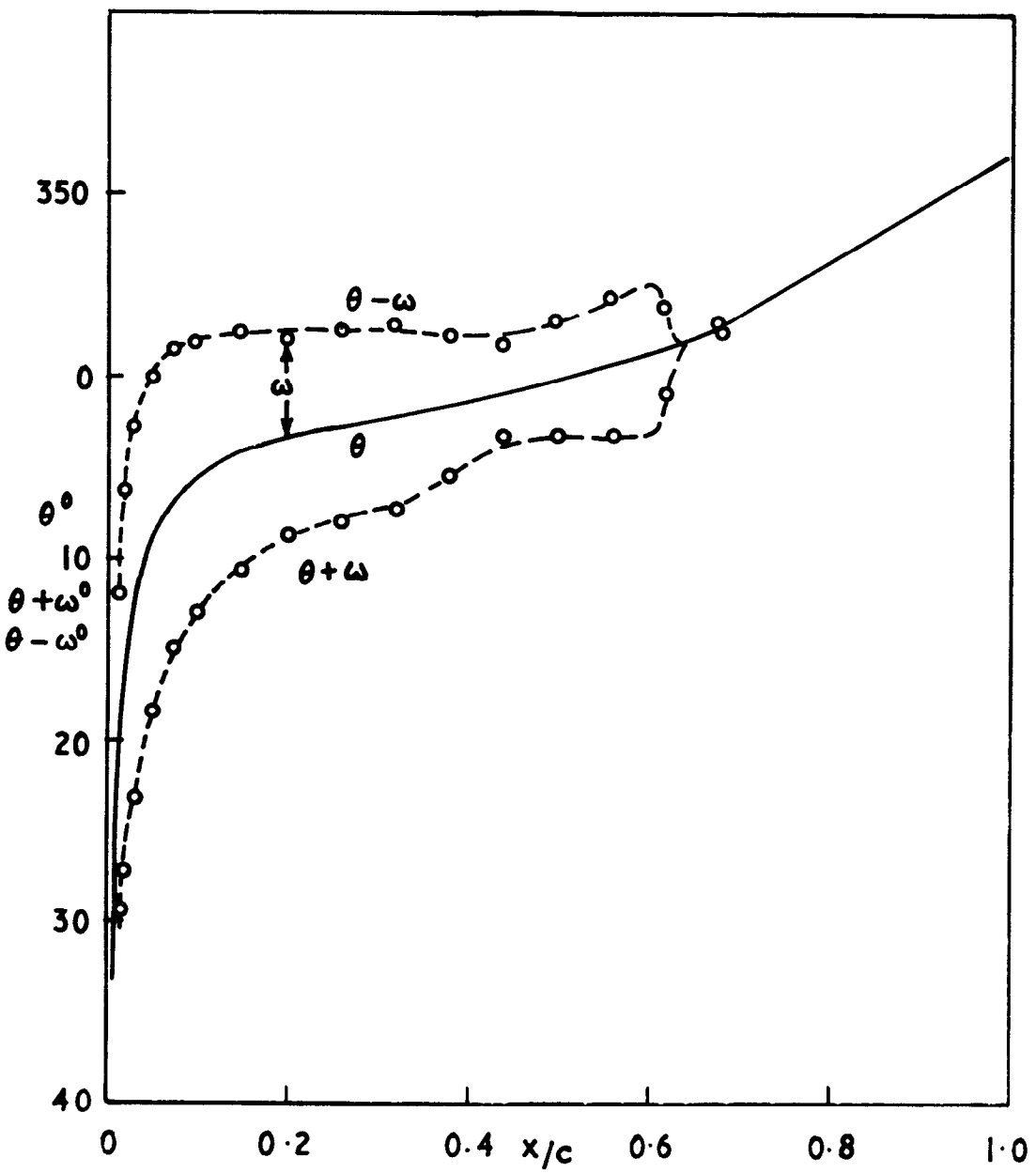

Aerofoil NPL 9510. Characteristics diagram

$M_\infty = 0{\cdot}785, \quad \alpha = 2^\circ$

31312
FIG.16.

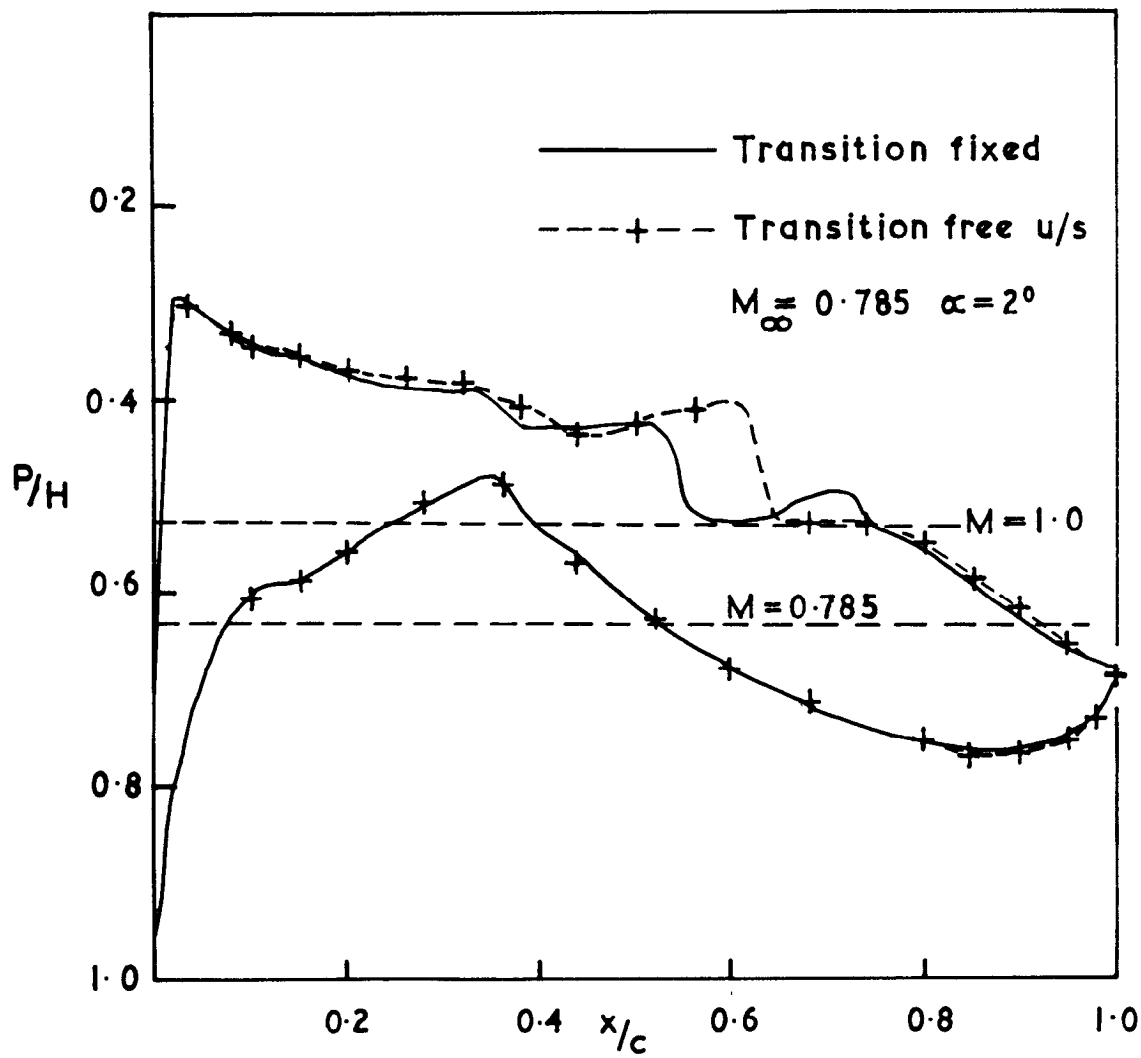

Aerofoil NPL 9510. Effect of upper surface carborundum band.

31312

FIG. 17

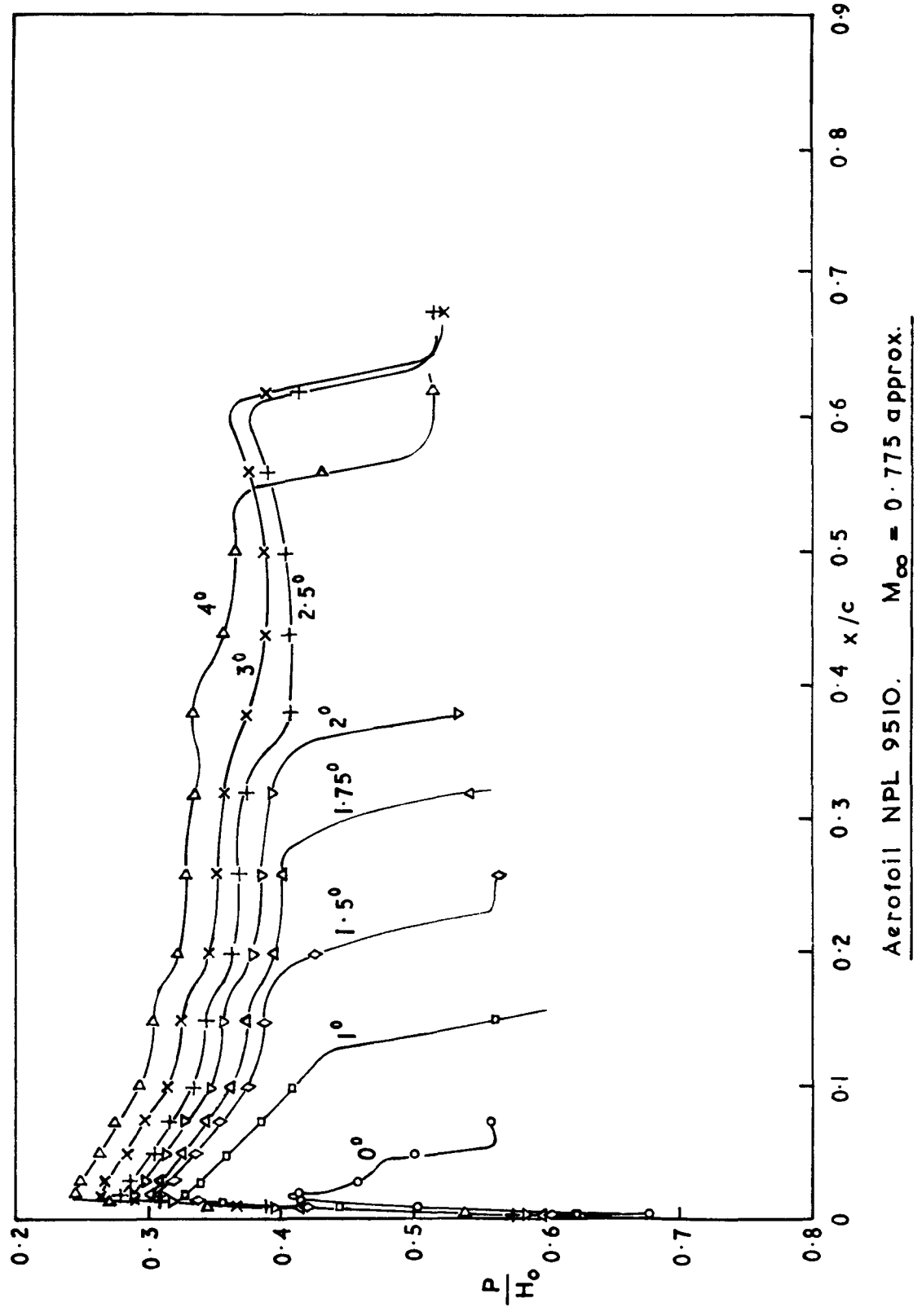

Aerofoil NPL 9510. $M_\infty = 0.775$ approx.

31312
FIG. 18

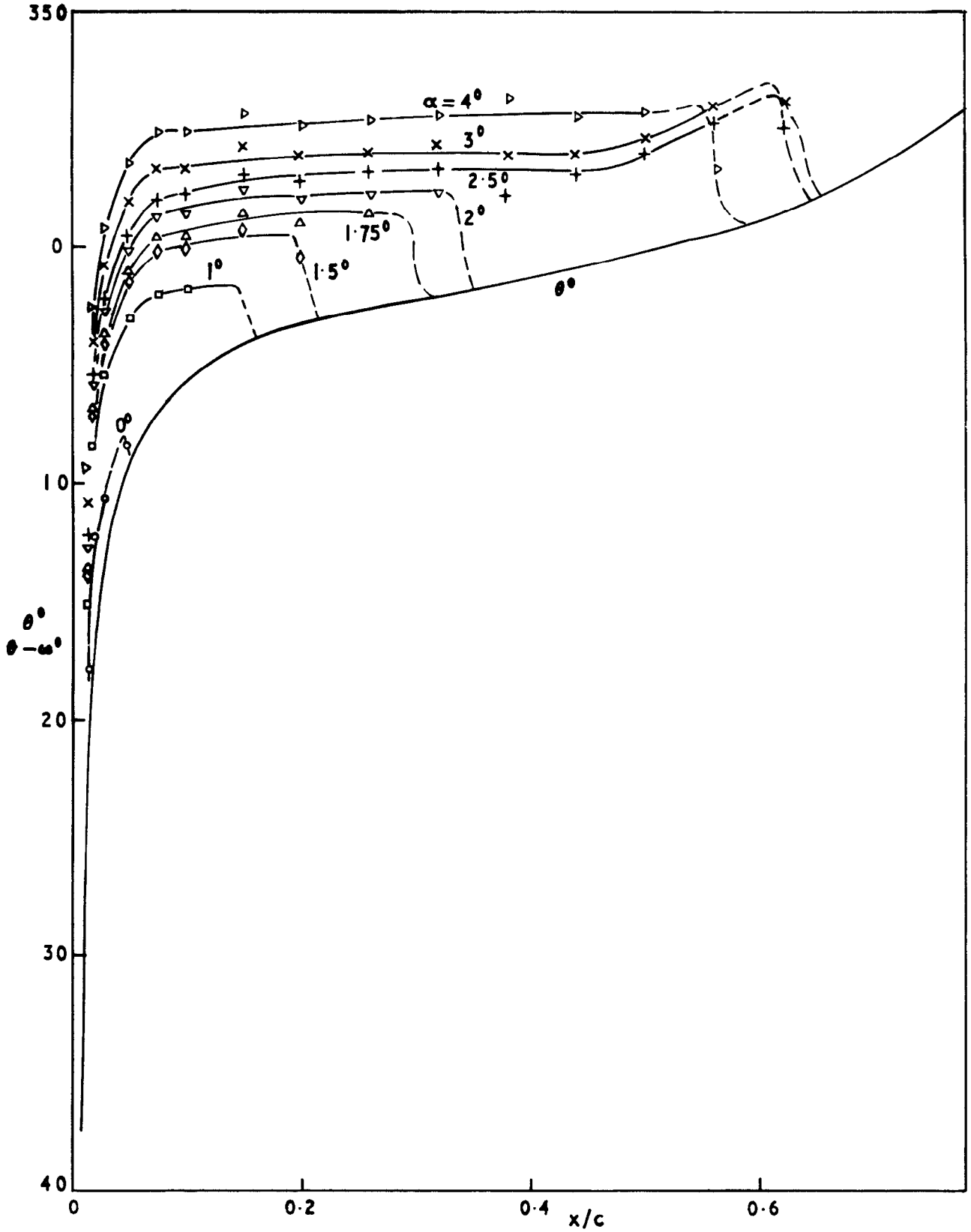

Aerofoil NPL 9510 M_∞ = 0·775 approx.

31312

FIG.19

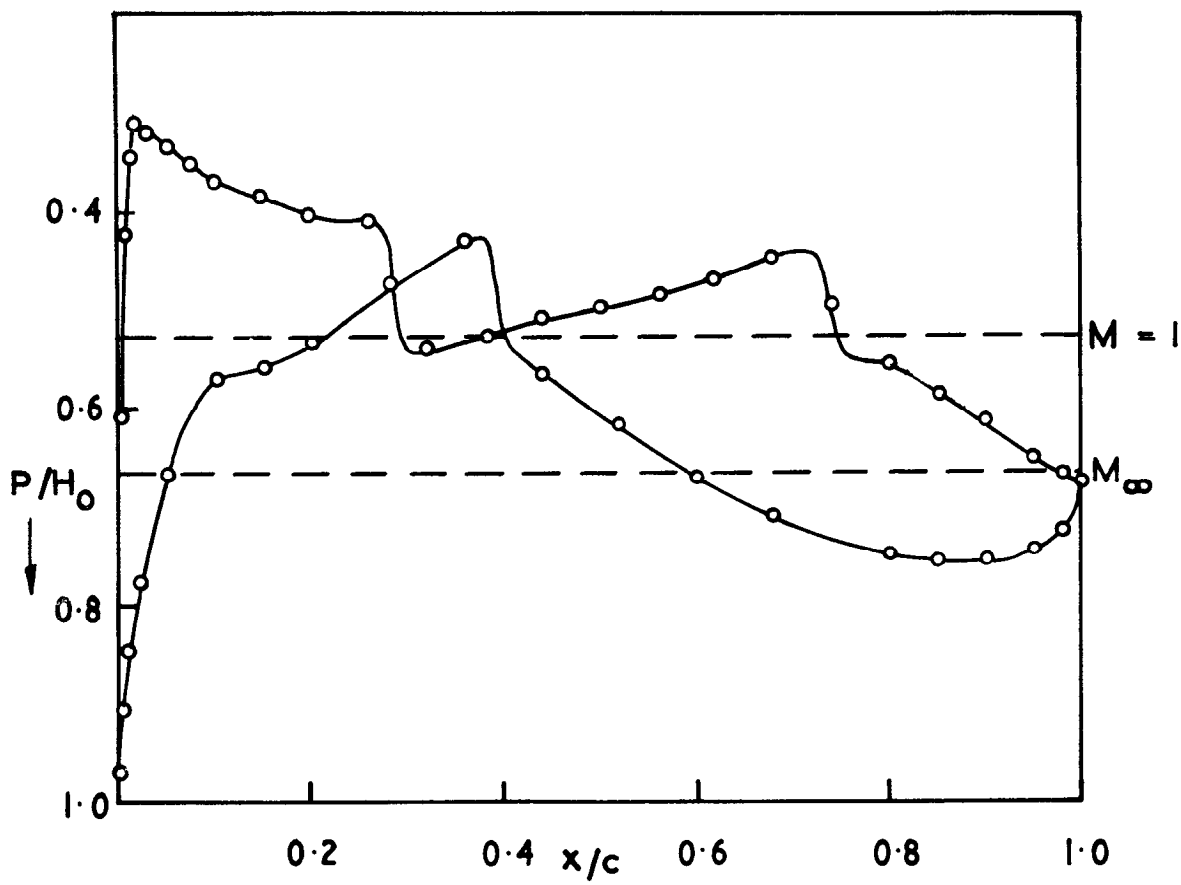

Aerofoil NPL 9510. $M_\infty = 0{\cdot}79$, $\alpha = 1{\cdot}5^\circ$.

ARC CP No.1292
July 1969
Hall, D.J., Quincey, V.G. and Lock, R.C.

SOME RESULTS OF WIND-TUNNEL TESTS ON AN AEROFOIL SECTION (NPL 9510) COMBINING A 'PEAKY' UPPER SURFACE-PRESSURE DISTRIBUTION WITH REAR LOADING

The paper describes experiments on a high-subsonic speed 'peaky' aerofoil section designed to have supersonic flow over a large part of its upper surface and heavy rear loading. At its optimum operating conditions the section showed a considerable increase in performance over a conventional 'rooftop' type, but there are a number of undesirable 'off-design' characteristics to be overcome before it can be practically useful.

ARC CP No.1292
July 1969
Hall, D.J., Quincey, V.G. and Lock, R.C.

SOME RESULTS OF WIND-TUNNEL TESTS ON AN AEROFOIL SECTION (NPL 9510) COMBINING A 'PEAKY' UPPER SURFACE-PRESSURE DISTRIBUTION WITH REAR LOADING

The paper describes experiments on a high-subsonic speed 'peaky' aerofoil section designed to have supersonic flow over a large part of its upper surface and heavy rear loading. At its optimum operating conditions the section showed a considerable increase in performance over a conventional 'rooftop' type, but there are a number of undesirable 'off-design' characteristics to be overcome before it can be practically useful.

ARC CP No.1292
July 1969
Hall, D.J., Quincey, V.G. and Lock, R.C.

SOME RESULTS OF WIND-TUNNEL TESTS ON AN AEROFOIL SECTION (NPL 9510) COMBINING A 'PEAKY' UPPER SURFACE-PRESSURE DISTRIBUTION WITH REAR LOADING

The paper describes experiments on a high-subsonic speed 'peaky' aerofoil section designed to have supersonic flow over a large part of its upper surface and heavy rear loading. At its optimum operating conditions the section showed a considerable increase in performance over a conventional 'rooftop' type, but there are a number of undesirable 'off-design' characteristics to be overcome before it can be practically useful.

DETACHABLE ABSTRACT CARDS

HER MAJESTY'S STATIONERY OFFICE

Government Bookshops

49 High Holborn, London WC1V 6HB
13a Castle Street, Edinburgh EH2 3AR
41 The Hayes, Cardiff CF1 1SW
Brazennose Street, Manchester M60 8AS
Southey House, Wine Street, Bristol BS1 2BQ
258 Broad Street, Birmingham B1 2HE
80 Chichester Street, Belfast BT1 4JY

Government publications are also available through booksellers

C.P. No. 1292

ISBN 011 470876 2